Noname manuscript No.
(will be inserted by the editor)

A Multi-Scale Model for the Intraseasonal Impact of the Diurnal Cycle of Tropical Convection

Qiu Yang · Andrew J. Majda

Received: date / Accepted: date

Abstract One of the crucial features of tropical convection is the observed variability on multiple spatiotemporal scales, ranging from cumulus clouds on the daily time scale over a few kilometers to intraseasonal oscillations over planetary scales. The diurnal cycle of tropical convection is a significant process but its large-scale impact is not well understood. Here we develop a multi-scale analytic model to assess the intraseasonal impact of planetary-scale inertial oscillations in the diurnal cycle. A self-contained derivation of a multi-scale model governing planetary-scale tropical flows on the daily and intraseasonal time scale is provided below, by following the derivation of systematic multi-scale models for tropical convection. This derivation demonstrates the analytic tractability of the model. The appeal of the multi-scale model developed here is that it provides assessment of eddy flux divergences of momentum and temperature and their intraseasonal impact on the planetary-scale circulation in a transparent fashion. Here we use it to study the intraseasonal impact of a model for the diurnal cycle heating with two local phase-lagged baroclinic modes with the congestus, deep, stratiform life cycle. The results show that during boreal summer the eddy flux divergence of temperature dominates in the northern hemisphere, providing significant heating in the middle troposphere of the northern hemisphere with large-scale ascent and cooling with subsidence surrounding this heating center. Due to the analytic tractability of the model, such significant eddy flux divergence of temperature is traced to meridional asymmetry of the diurnal cycle heating. In an ideal zonally symmetric case, the resulting planetary-scale circulation on the intraseasonal time scale during boreal summer is characterized by ascent in the northern hemisphere, southward motion in the upper troposphere, descent around the equator and northward motion in the lower troposphere. The intraseasonal impact of the diurnal cycle on the planetary scale also includes negative potential temperature anomalies in the lower troposphere, which suggests convective triggering in the tropics. Furthermore, a fully coupled model for the intraseasonal impact of the diurnal cycle on the Hadley cell shows that the overturning motion induced by the eddy flux divergences of momentum and temperature from the diurnal cycle can strengthen the upper branch of the winter cell of the Hadley circulation, but weaken the lower branch of the winter cell. The corresponding eddy fluxes from the diurnal cycle are very weak for the equinox case with symmetric meridional profiles and eddy momentum fluxes are small for all scenarios considered here.

Keywords Diurnal cycle · Upscale fluxes · Intraseasonal impact · Multi-scale asymptotics

1 Introduction

The diurnal cycle of solar radiation has a major impact on atmospheric flow. Particularly, it induces significant variability in tropical storms and the associated winds and precipitation over land and ocean areas adjacent to continents. Early investigations of the diurnal variability of tropical precipitation date

Qiu Yang
Courant Institute of Mathematical Sciences, Department of Mathematics and Center for Atmosphere Ocean Science, New York University, New York, New York
Tel.: +1(646)620-6686
E-mail: yangq@cims.nyu.edu

Andrew J. Majda
Courant Institute of Mathematical Sciences, Department of Mathematics and Center for Atmosphere Ocean Science, New York University, New York, New York

back to 1920s [31]. The development of satellite measurements and computers has triggered more work such as the GARP Atlantic Tropical Experiment (GATE) [27,13,1], the European Union Cloud Archive User Service (CLAUS) project [39] and the Tropical Rainfall Measuring Mission (TRMM) [40,29,36,34], leading the community to have a better understanding of the diurnal variability of tropical convection and precipitation over land and oceans. Kikuchi and Wang in 2008 [19] confirmed the persistence of the diurnal variation of tropical precipitation by using empirical orthogonal functions(EOFs) and two complementary TRMM datasets(3B42 and 3G68) for 1998-2006. Their results show that the amplitude of the diurnal variability of tropical precipitation in the continental regime is much stronger than that in the oceanic regime. Meanwhile it was found [19] that the diurnal range (DR), which is defined as the climatological daily maximum precipitation minus daily minimum precipitation, has different meridional spatial patterns in different seasons. For the annual mean of tropical precipitation, the equatorial continental regime has relatively large DR, such regime is observed at the Indonesian Maritime Continent and South America around the equator. For the June July August(JJA) mean of tropical precipitation, the DR is relatively large on the continents but in the northern hemisphere such as South Asia, the Indonesian Maritime Continent and Mexico.

The representation of the diurnal variability of tropical precipitation is a major unsolved problem and very crucial for global weather forecast and climate models. For example, present-day computer general circulation models(GCM) typically poorly represent the Madden-Julian oscillation(MJO) near the Indonesian Maritime Continent [35]. One possible shortcoming is the inadequate treatment of the diurnal cycle and its impact on the intraseasonal variability of atmospheric flow. In fact, current global and regional numerical models of weather and climate have difficulty in reproducing the diurnal variability of tropical precipitation [30,39,6,37]. Nevertheless, both the diurnal cycle of tropical convection and MJO simulation have been improved a lot with superparameterization [15,33,2]. In a theoretical direction, models utilizing three cloud types (congestus, deep and stratiform) based on the first two baroclinic modes of vertical structure plus a boundary layer mode have been built [16–18], successfully reproducing several features of a realistic diurnal cycle of tropical precipitation over land and oceans [7–9].

The goal of this paper is to build an analytic multi-scale model to assess the intraseasonal impact of the diurnal cycle of tropical convection. Compared with the numerical models, the analytic multi-scale model developed here has the appeal that it is analytically tractable and relatively simple but sill consistent with several key features of the observations such as the diurnal cycle heating associated with the cloud life cycle. Furthermore, there are eddy flux divergences of momentum and temperature in the planetary/intraseasonal scale equations, which shows that the model is able to assess upscale effects spatially from the synoptic scale to the planetary scale and temporally from the daily time scale to the intraseasonal time scale in an idealized fashion. Several related studies in the framework of the intraseasonal planetary equatorial synoptic dynamics (IPESD) model [25] consider the central role of organized vertically tilted synoptic-scale circulations in reproducing key features of MJO across multiple spatial scales [24,3,4]. The IPESD model also involves two spatial scales (the synoptic scale and the planetary scale) but only one temporal scale (the intraseasonal time scale). In contrast, here the analytic multi-scale model is used to assess upscale effects across multiple temporal scales, that is, the intraseasonal impact of the diurnal cycle.

Through systematic multi-scale asymptotics following [23], four systems of equations involving physical variables on different spatiotemporal scales are derived. The model for the diurnal cycle is one of those systems, involving all physical variables on the planetary scale and daily time scale. Since there is a general heating term in the thermal equation in this model, we prescribe this heating profile to mimic the latent heat which is released during tropical precipitation in the diurnal cycle. Here we utilize the first two baroclinic models of vertical structure to characterize organized tropical convection based on three cloud types(congestus, deep convective and stratiform) in the free troposphere, which was first introduced in a simple multicloud model [16–18]. The second system of equations derived in the paper is utilized as a model for the planetary/intraseasonal scale circulation, which includes eddy flux divergences of momentum and temperature from the model for the diurnal cycle. Thus, the resulting circulation response on the planetary/intraseasonal scales describes the intraseasonal impact of the diurnal cycle. The results show that the eddy flux divergence of temperature during boreal summer is much stronger than that during equinox, which suggests that the significant intraseasonal impact of the diurnal cycle is traced to the meridional asymmetry of the diurnal cycle heating profile in the first two baroclinic modes. In general, the dimensionless magnitude of the eddy flux divergence of temperature due to the diurnal cycle is much larger than that of the eddy flux divergence of momentum. In an ideal zonally symmetric case, the resulting steady state circulation on the planetary/intraseasonal scales during boreal summer is characterized by a circulation cell around the equator. By coupling this system with the model for

the Hadley cell, we conclude that the intraseasonal impact of the diurnal cycle can strengthen the upper branch of the winter cell of the Hadley circulation but weaken the lower branch of the winter cell of the Hadley circulation.

The rest of this paper is organized as follows. The basic nondimensional equations and multi-scale asymptotics are summarized in section 2. In that section, we start from the primitive equations and derive four systems on multiple spatiotemporal scales by utilizing the multi-scale asymptotic method. The model for the diurnal cycle is developed in section 3. In that section, we prescribe the diurnal cycle heating in meridionally symmetric and asymmetric profiles to mimic the equinox case and boreal summer case separately. Section 4 is used to assess the intraseasonal impact of the diurnal cycle of tropical convection on the planetary/intraseasonal scales in an ideal zonally symmetric case. There are two planetary/intraseasonal scale circulation systems, which involve meridional and vertical velocity components in different orders. The leading-order system can be used to describe the Hadley cell [4]. The second order system can be understood as the planetary-scale circulation response to the intraseasonal impact of the diurnal cycle, since in this system there are eddy flux divergences of the momentum and temperature from the model of the diurnal cycle in section 3. Here we first consider the intraseasonal impact of the diurnal cycle without the advection effects of the Hadley cell. Then we consider a fully coupled system for the planetary/intraseasonal scale circulation advected by the Hadley cell. Finally, a concluding discussion is given in section 5. Technical details for the derivation of the multi-scale model, explicit formulas of eddy flux divergences, and the numerical methods, used for solving the model equations, are summarized in the Appendix.

2 Basic Nondimensional Equations and Multi-Scale Asymptotics

Tropical convection is organized on a hierarchy of spatiotemporal scales such as the tropical super clusters within intraseasonal variations over the western Pacific [28,11,38]. Here we want to study the effect of the diurnal tropical convection on the atmospheric flow, by utilizing simplified multiscale asymptotic models. The fundamental model for the dynamical behavior of atmospheric flow consists of the hydrostatic, anelastic Euler equations on an equatorial β-plane, which are the appropriate equations for large-scale phenomenon in the tropical troposphere

$$\frac{D}{Dt}u - yv = -p_x + S_u \tag{1a}$$

$$\frac{D}{Dt}v + yu = -p_y + S_v \tag{1b}$$

$$\frac{D}{Dt}\theta + N^2 w = S_\theta \tag{1c}$$

$$p_z = \theta \tag{1d}$$

$$(\rho u)_x + (\rho v)_y + (\rho w)_z = 0 \tag{1e}$$

where $\frac{D}{Dt} = \frac{\partial}{\partial t} + u\frac{\partial}{\partial x} + v\frac{\partial}{\partial y} + w\frac{\partial}{\partial z}$ is the three dimensional advective derivative. We use the same nondimensionalization as in earlier work [4,23]. Both the density $\rho = \rho(z)$ and the buoyancy frequency $N = N(z)$ only depend on the height in the troposphere. The Eqs. (1a-1e) have been nondimensionalized so that time scale is measured in units of the equatorial time scale $T_E = (c\beta)^{-1/2} \approx 8.3h$, the horizontal length scale is in units of the equatorial deformation radius $L_E = (c/\beta)^{1/2} = 1500km$, the vertical length scale is in units of the troposphere height divided by π, $H = H_T/\pi \approx 5km$. Here c is defined as the dry Kelvin wave speed and β denotes the Rossby parameter in the Beta plane approximation. The horizontal velocity is scaled to the dry Kelvin/gravity wave speed $c = 50m/s$ and the vertical velocity is scaled to this wave speed c multiplied by the aspect ratio between the vertical length scale and the horizontal length scale, $(H/L_E)\,c \approx 0.16m/s$. The potential temperature scale is equal to the mean potential temperature difference over one unit of the vertical scale H, $\Theta = N^2\theta_0 H/g = 15.3K$, where we assume a constant buoyancy frequency $N = 10^{-2}s^{-1}$ and a mean potential temperature $\theta_0 = 300K$. N^2 has units s^{-2} and is referred as stratification. In Eq. 1c, θ denotes the potential temperature deviation from the mean potential temperature. The free troposphere occupies the domain $-20 * 10^3 km \le x \le 20 * 10^3 km$,

Table 1 The dimensional units for all physical variables and some constant parameters. Here square brackets mean the value of one unit of the dimensionless variables corresponding to the given scale.

Physical quantity	Mathematical symbol	Value
Froude number	ϵ	0.1
Gravity wave speed	c	$50m/s$
Brunt-vaisala frequency	N	$0.01s^{-1}$
Troposphere height	H_T	$16km$
Equatorial time scale	T_E	$(c\beta)^{-1/2} = 8.3h$
Equatorial deformation radius	L_E	$(c/\beta)^{1/2} = 1500km$
Synoptic scale	$[x, y]$	$L_E = 1500km$
vertical scale	$[z]$	$H_T/\pi = 5km$
Daily scale	$[t]$	$T_E = 8.3h$
Zonal planetary scale	$[X]$	$L_P = L_E/\epsilon = 15000km$
Intraseasonal scale	$[T]$	$T_I = T_E/\epsilon = 3.5day$

$-5 * 10^3 km \leq y \leq 5 * 10^3 km$, $0km \leq z \leq 16km$. The dimensional units for all physical variables and some constant parameters are summarized in Table 1.

Here the zonal and meridional momentum forcings S_u, S_v include momentum dissipation. To parameterize the momentum dissipation, we employ a linear drag law closure in the form of $S_u = -du$,$S_v = -dv$. The parameter d contains the the equivalent linear damping time scale of the momentum dissipation. Here the dissipation time is ascribed to cumulus drag, which has been estimated to be about 5 days from observations of large-scale tropical flows [20,32]. Since the equatorial time scale is $T_E = (c\beta)^{-\frac{1}{2}} \approx 8.3h \approx \frac{1}{3}day$, we can find the dimensionless value of the dissipation rate $d = \frac{1}{15} = 0.07$. Thus we can rewrite the horizontal momentum forcings as$-\epsilon du + S_u$ in Eq. (1a) and $-\epsilon dv + S_v$ in Eq. (1b), where $d = 0.7$ and S_u, S_v account for all extra forcings.

The thermal forcing S_θ includes radiative damping. Here we use a linear Newtonian cooling law $S_\theta = -d_\theta \theta$. Considering the observational estimates for the cooling time are of the order 15 days and the equatorial time scale is $T_E = (c\beta)^{-\frac{1}{2}} \approx 8.3h \approx \frac{1}{3}day$, we can find the dimensionless value of the radiative damping rate $d_\theta = \frac{1}{45} = 0.023$. Thus we rewrite the thermal forcing as $-\epsilon d_\theta \theta + S_\theta$ in Eq. (1c), where $d_\theta = 0.23$ and S_θ accounts for all extra forcings such as latent heat release during tropical precipitation.

By incorporating the momentum dissipation and radiative damping terms into the primitive equations (1a-1e), we can rewrite them as

$$\frac{D}{Dt}u - yv = -p_x - \epsilon du + S_u \tag{2a}$$

$$\frac{D}{Dt}v + yu = -p_y - \epsilon dv + S_v \tag{2b}$$

$$\frac{D}{Dt}\theta + N^2 w = -\epsilon d_\theta \theta + S_\theta \tag{2c}$$

$$p_z = \theta \tag{2d}$$

$$(\rho u)_x + (\rho v)_y + (\rho w)_z = 0 \tag{2e}$$

The derivation of the multi-scale model in this paper is based on the following three basic assumptions [23]:

Assumption 1: Low Froude number. Since the reference flow speed $c = 50m/s$ is much faster than the real flow speed on the synoptic or larger scales in the tropical troposphere, the Froude number, which is defined as the ratio between the typical horizontal velocity magnitude and the basic wave speed $F_r = U/c = \epsilon$, is assumed to be small. The dimensionless horizontal flow field $\mathbf{u}_h = (u, v)$ is rewritten as $\mathbf{u}_h = \epsilon \mathbf{u}_{h,1}$, where one dimensionless unit of the magnitude of $\mathbf{u}_{h,1}$ means $\epsilon c = 5m/s$.

Assumption 2: Weak temperature gradient. The potential temperature deviation has be nondimensionalized as the temperature scale ($15K$), the mean potential temperature difference over one unit of the vertical length scale. However, the real potential temperature deviation θ, whose value is several kelvin in tropical troposphere [21,41], is much smaller than that. Thus the dimensionless potential temperature deviation can be rewritten as $\theta = \epsilon\theta_1$, where one dimensionless unit of θ_1 means $\epsilon\Theta = 1.5K$.

Assumption 3: Although the momentum forcing S_u, S_v and the thermal forcing S_θ have been nondimensionalized to $150m/s/day$, $45K/day$, the measured atmospheric flow is much weaker than the corresponding dimensional units. For example, the measured heating associated with latent heat release in the tropics on the synoptic and larger scales is only several Kelvin per day. Thus we can rewrite the momentum and thermal forcings as $S_u = \epsilon S_{u,1}, S_\theta = \epsilon S_{\theta,1}$, where one dimensionless unit of $S_{u,1}$ means $15m/s/day$. and that of $S_{\theta,1}$ means $4.5K/day$.

The ansatz we use in this multi-scale model is that the solutions for all physical variables can be approximated by functions which vary on two zonal spatial scales and two temporal scales. Specifically, these two zonal spatial scales are the synoptic scale ($L_E = 1500km$) and the planetary scale ($L_P = 15000km$). These two temporal scales are the daily time scale($T_E = 8.3h$) and the intraseasonal time scale($T_I = 3.5days$). Since ten units of this time scale span more than one month, T_I is an intraseasonal time scale. In general, for an arbitrary function f such as physical variables u, v, w, p, θ, we can have

$$f(x,t,y,z) = f^\epsilon(x,X,t,T,y,z) \tag{3}$$

where we introduce the planetary-scale zonal variable $X = \epsilon x$, and the intraseasonal time scale variable $T = \epsilon t$, and y, z are on the synoptic scale. The implicit meaning in the ansatz (3) is that all physical variables can vary an amount of order one but no more than order one if any of the independent variables x, X, t, T, y, z vary an amount of order one, in order to guarantee the validity of the multi-scale asymptotics.

By assuming multi-scale solutions as Eq. (3), the zonal and time derivatives are given by chain rule

$$\frac{\partial f^\epsilon}{\partial x} + \epsilon\frac{\partial f^\epsilon}{\partial X},\ \frac{\partial f^\epsilon}{\partial t} + \epsilon\frac{\partial f^\epsilon}{\partial T} \tag{4}$$

In order to consider averages of physical variables on the small spatial and temporal scales, we use the following averaging operators

$$\bar{f}(X,t,T,y,z) = \lim_{L\to\infty}\frac{1}{2L}\int_{-L}^{L} f(x,X,t,T,y,z)\,dx \tag{5}$$

$$\langle f\rangle(x,X,T,y,z) = \lim_{T^*\to\infty}\frac{1}{2T^*}\int_{-T^*}^{T^*} f(x,X,t,T,y,z)\,dt \tag{6}$$

For an arbitrary function f, we can have its zonal spatial average $\bar{f}$, therefore $f = \bar{f} + f'$ and f' satisfies $\bar{f}' = 0$. Similarly, we can have its temporal average $\langle f\rangle$, therefore $f = \langle f\rangle + \tilde{f}$ and $\tilde{f}$ satisfies $\left\langle \tilde{f} \right\rangle = 0$. In order to guarantee the validity of multi-scale asymptotics, all physical variables need to satisfy the sublinear growth condition, thus secular growth in space and time can be avoid and we have the following conditions $\overline{\frac{\partial}{\partial x}f} = 0, \left\langle \frac{\partial}{\partial t}f \right\rangle = 0$.

With the assumptions of the low Froude number, the weak temperature gradient and that for momentum and thermal forcing magnitude, we are ready to write down the ansatz for all physical variables on multiple spatiotemporal scales [25, 23]

$$g = \epsilon\left[g'(x,X,t,T,y,z) + \bar{g}(X,t,T,y,z)\right] + \epsilon^2 g_2,\ g \in \{u,v,w,\theta,p,S_u,S_v,S_\theta\} \tag{7}$$

Now we can derive the multi-scale model, the detailed steps of the derivation can be found in Appendix A.

2.1 The planetary-scale system

Substituting the ansatz (7) into Eqs. (2a-2e) and collecting all terms at the leading order yields a linear system. Now we do zonal spatial averaging over the synoptic scale, and get *the planetary-scale system*

$$\bar{u}_t - y\bar{v} = \bar{S}_u \tag{8a}$$

$$\bar{v}_t + y\bar{u} = -\bar{p}_y + \bar{S}_v \tag{8b}$$

$$\bar{\theta}_t + N^2\bar{w} = \bar{S}_\theta \tag{8c}$$

$$\bar{p}_z = \bar{\theta} \tag{8d}$$

$$\bar{v}_y + \frac{1}{\rho}\left(\rho\bar{w}\right)_z = 0 \tag{8e}$$

which describes the planetary-scale flow field. This system includes the planetary-scale inertial effects of equatorial rotation. A crucial property of this system is that it is a linear system without advective effects since the weak advection terms are at the second order. After zonal spatial averaging, this flow field is zonally symmetric on the synoptic scale. In addition, since there is no derivative with respect to the planetary scale X , it can be regarded as a frozen parameter in the the resulting flow field. Also, one dimensionless unit of horizontal velocity corresponds to $5m/s$ and that of potential temperature deviation corresponds to $1.5K$. Therefore, this system allows the momentum forcing to be roughly $15m/s/day$ and the thermal forcing to be roughly $4.5K/day$.

2.2 The synoptic-scale system

By subtracting *the planetary-scale system* (8a-8e) from the leading-order asymptotic equations, we can derive *the synoptic-scale system* [23]

$$u_t^{'} - yv^{'} = -p_x^{'} + S_u^{'} \tag{9a}$$

$$v_t^{'} + yu^{'} = -p_y^{'} + S_v^{'} \tag{9b}$$

$$\theta_t^{'} + N^2 w^{'} = S_\theta^{'} \tag{9c}$$

$$p_z^{'} = \theta^{'} \tag{9d}$$

$$u_x^{'} + v_y^{'} + \frac{1}{\rho}\left(\rho w^{'}\right)_z = 0 \tag{9e}$$

which describes the synoptic-scale fluctuations of the flow field. These synoptic-scale fluctuating flows are characterized by linear equations without advective effects. Also, the momentum dissipation and radiative damping do not directly affect these synoptic-scale fluctuating flows since they are at the second order.

2.3 The leading-order planetary scale system on the intraseasonal time scale

Since the daily time scale t is the fast time scale compared with the intraseasonal time scale T, it is required that $\langle \partial g/\partial t \rangle = 0$ for any bounded function g to guarantee the validity of the asymptotics. We do time averaging on Eqs. (8a,8c,8e) , and get *the leading-order planetary scale system on the intraseasonal time scale* [4]

$$-y\left\langle \bar{v} \right\rangle = \left\langle \bar{S}_u \right\rangle \tag{10a}$$

$$N^2\left\langle \bar{w} \right\rangle = \left\langle \bar{S}_\theta \right\rangle \tag{10b}$$

$$\left(\left\langle \bar{v} \right\rangle\right)_y + \frac{1}{\rho}\left(\rho\left\langle \bar{w} \right\rangle\right)_z = 0 \tag{10c}$$

Since the meridional velocity $\langle \bar{v} \rangle$ on the planetary/intraseasonal scales is directly determined by the zonal momentum forcing $\left\langle \bar{S}_u \right\rangle$ and the vertical velocity $\langle \bar{w} \rangle$ on the planetary/intraseasonal scales is directly determined by $\left\langle \bar{S}_\theta \right\rangle$, there exists a constraint if we combine Eqs. (10a,10b) with the incompressibility condition (10c)

$$\left(\frac{\left\langle \bar{S}_u \right\rangle}{y}\right)_y = \frac{1}{\rho}\left(\rho\frac{\left\langle \bar{S}_\theta \right\rangle}{N^2}\right)_z \tag{11}$$

Intuitively, this is not an unphysical requirement since a steady climatology requires a careful balance between the zonal momentum forcing and the thermal forcing. Also, if we do time averaging on Eqs. (8b,20) , we can get

$$y\left\langle \bar{u} \right\rangle = -\left\langle \bar{p} \right\rangle_y + \left\langle \bar{S}_v \right\rangle \tag{12}$$

$$\left\langle \bar{p} \right\rangle_z = \left\langle \bar{\theta} \right\rangle \tag{13}$$

which are the geostrophic balance in the meridional direction if $\left\langle \bar{S}_v \right\rangle = 0$ and the hydrostatic balance for the leading-order terms $\left\langle \bar{p} \right\rangle, \left\langle \bar{\theta} \right\rangle$.

2.4 The planetary-scale system on the daily time scale

Then we can further divide each planetary-scale physical variable into a long-time average and a fluctuation variable, that is $\bar{g} = \langle \bar{g} \rangle + \tilde{\bar{g}}$ and $\tilde{\bar{g}}$ satisfies $\langle \tilde{\bar{g}} \rangle = 0$. By subtracting the time mean equations (10a-10c, 12, 13) on the planetary/intraseasonal scales from Eqs. (8a-8e), we derive *the planetary-scale system on the daily time scale*

$$\tilde{\bar{u}}_t - y\tilde{\bar{v}} = \tilde{\bar{S}}_u \tag{14a}$$

$$\tilde{\bar{v}}_t + y\tilde{\bar{u}} = -\tilde{\bar{p}}_y + \tilde{\bar{S}}_v \tag{14b}$$

$$\tilde{\bar{\theta}}_t + N^2\tilde{\bar{w}} = \tilde{\bar{S}}_\theta \tag{14c}$$

$$\tilde{\bar{p}}_z = \tilde{\bar{\theta}} \tag{14d}$$

$$\tilde{\bar{v}}_y + \frac{1}{\rho}\left(\rho\tilde{\bar{w}}\right)_z = 0 \tag{14e}$$

which describes the daily time scale modulation of the planetary-scale flow. These equations are linear and do not have advection terms. Also, the flow does not depend on the zonal synoptic scale. More importantly, since all physical variables vanish after the time averaging $\langle \tilde{\bar{g}} \rangle = 0$, this system is a good candidate for the planetary-scale equatorial inertial oscillations to mimic the diurnal cycle of tropical convection. We model the diurnal cycle through this system in section 3.

2.5 The second-order planetary scale system on the intraseasonal time scale

Now we consider the asymptotic expansion of the primitive equations at the second order following [23]. After zonal spatial and temporal averaging on the zonal momentum equation (2a), the thermal equation (2c), and the mass conservation (2e), all terms at the second order are collected and form *the second-order planetary scale system on the intraseasonal time scale*, if they are combined with Eqs. (12-13)

$$\frac{D}{DT}\left\langle \bar{u} \right\rangle - y\left\langle \bar{v}_2 \right\rangle = -\left\langle \bar{p} \right\rangle_X - d\left\langle \bar{u} \right\rangle - \frac{\partial}{\partial y}\left\langle \overline{v'u'} \right\rangle - \frac{1}{\rho}\frac{\partial}{\partial z}\left(\rho\left\langle \overline{w'u'} \right\rangle\right) - \frac{\partial}{\partial y}\left\langle \tilde{\bar{v}}\tilde{\bar{u}} \right\rangle - \frac{1}{\rho}\frac{\partial}{\partial z}\left(\rho\left\langle \tilde{\bar{w}}\tilde{\bar{u}} \right\rangle\right) + \left\langle \bar{S}_{u,2} \right\rangle \tag{15a}$$

$$y\left\langle \bar{u} \right\rangle = -\left\langle \bar{p} \right\rangle_y + \left\langle \bar{S}_v \right\rangle \tag{15b}$$

$$\frac{D}{DT}\left\langle \bar{\theta} \right\rangle + N^2\left\langle \bar{w}_2 \right\rangle = -d_\theta\left\langle \bar{\theta} \right\rangle - \frac{\partial}{\partial y}\left\langle \overline{v'\theta'} \right\rangle - \frac{1}{\rho}\frac{\partial}{\partial z}\left(\rho\left\langle \overline{w'\theta'} \right\rangle\right) - \frac{\partial}{\partial y}\left\langle \tilde{\bar{v}}\tilde{\bar{\theta}} \right\rangle - \frac{1}{\rho}\frac{\partial}{\partial z}\left(\rho\left\langle \tilde{\bar{w}}\tilde{\bar{\theta}} \right\rangle\right) + \left\langle \bar{S}_{\theta,2} \right\rangle \tag{15c}$$

$$\left\langle \bar{p} \right\rangle_z = \left\langle \bar{\theta} \right\rangle \tag{15d}$$

$$\langle \bar{u} \rangle_X + \langle \bar{v}_2 \rangle_y + \frac{1}{\rho} \left(\rho \langle \bar{w}_2 \rangle \right)_z = 0 \tag{15e}$$

where $\frac{D}{DT} = \frac{\partial}{\partial T} + \langle \bar{v} \rangle \frac{\partial}{\partial y} + \langle \bar{w} \rangle \frac{\partial}{\partial z}$, this system is advected by the leading-order meridional and vertical velocity in section 2.3. This system describes the evolution of $\langle \bar{u} \rangle, \langle \bar{p} \rangle, \langle \bar{\theta} \rangle, \langle \bar{v}_2 \rangle, \langle \bar{w}_2 \rangle$ on the planetary/intraseasonal scales. The difference between this system and the leading-order planetary scale system on the intraseasonal time scale (Eqs. 10a-10c) is that the zonal momentum equation and thermal equation here are forced by eddy flux divergences of momentum and temperature from the synoptic scale and the daily time scale, as shown in the right side of Eqs. (15a, 15c). There are two pieces of upscale flux divergences in each equation. The first piece corresponds to the spatial upscale feedback from the synoptic scale to the planetary scale and can be further divided into meridional and vertical components. The second piece corresponds to the temporal upscale feedback from the daily time scale to the intraseasonal time scale and also can be divided into meridional and vertical components. These two pieces of eddy flux divergences of momentum and temperature force the planetary/intraseasonal scale flows (Eqs. 15a-15e) in a linear way. According to the physical observation that the dissipation time scales of the momentum damping and the radiative damping are both on the intraseasonal time scale, the planetary/intraseasonal scale circulation anomalies described here are subject to this momentum dissipation and radiative damping. This system includes not only the eddy flux divergences of momentum and temperature from the synoptic scale, which have already been explored in the IPESD model [25,24,3,4], but also those from the daily time scale, providing a more general framework to assess upscale effects.

3 A Model for the Diurnal Cycle and Upscale Fluxes

The diurnal variability of tropical precipitation over land and oceans has been summarized and clarified in [19]. By applying empirical orthogonal functions (EOF) analysis to two TRMM datasets, they confirmed the persistence of the diurnal cycle of tropical precipitation whose amplitude is relatively large in the continental regime and weak in the oceanic regime. Furthermore, the significant variability of tropical precipitation due to the diurnal cycle of solar heating is examined in the context of simple models for tropical convection [7–9]. These models utilize three cloud types(congestus, deep and stratiform) to characterize organized tropical convection. Since the latent heat can drive the atmospheric flow through thermodynamics, the diurnal cycle of tropical precipitation can induce the diurnal variability of the flow field in the tropical troposphere. In this section, we build a model for the diurnal cycle, and discuss the planetary-scale inertial oscillations on the daily time scale as well as the resulting upscale fluxes on the planetary/intraseasonal scale.

We start from *the planetary-scale system on the daily time scale*(14a-14e) and assume that there is only thermal forcing $\tilde{\bar{S}}_\theta$ associated with latent heat release, but no momentum forcing $\tilde{\bar{S}}_u, \tilde{\bar{S}}_v$. Also, we assume the buoyancy frequency N^2 and the density ρ to be constant so that their dimensionless values are equal to 1 and the Boussinesq approximation is used. Although the density profile in the realistic atmosphere changes dramatically with the height, such distinction does not change the qualitative conclusion and makes for more streamlined notation.

$$\tilde{\bar{u}}_t - y\tilde{\bar{v}} = 0 \tag{16a}$$

$$\tilde{\bar{v}}_t + y\tilde{\bar{u}} = -\tilde{\bar{p}}_y \tag{16b}$$

$$\tilde{\bar{\theta}}_t + \tilde{\bar{w}} = \tilde{\bar{S}}_\theta \tag{16c}$$

$$\tilde{\bar{p}}_z = \tilde{\bar{\theta}} \tag{16d}$$

$$\tilde{\bar{v}}_y + \tilde{\bar{w}}_z = 0 \tag{16e}$$

here we assume rigid lid boundary conditions at top and bottom of the troposphere

$$\tilde{\bar{w}}\left(x, X, t, T, y, z\right) |_{z=0,\pi} = 0 \tag{17}$$

where in dimensionless form $z = 0$ represents the surface of the earth and $z = \pi$ represents the top of the troposphere.

Since we use the thermal forcing $\tilde{\tilde{S}}_\theta$ in Eq. (16c) to represent the latent heat release during precipitation from clouds, a good cloud model can provide an appropriate heating profile. For example, the multicloud model convective parameterizations [16–18] based on three cloud types (congestus, deep and stratiform) have been revealed to be very useful in reproducing key features of organized convection and tropical precipitation in the continental regime [8]. These three cloud types serve to provide the bulk of tropical precipitation and the main source of latent heat in the troposphere. In detail, cumulus congestus clouds heat the lower troposphere through latent heat release and cool the upper troposphere due to detrainment and the high reflectivity at the tops of clouds. Deep convective clouds warm and dry the entire troposphere, and release the majority of tropical precipitation. Stratiform clouds warm the upper troposphere through precipitation and cool the lower troposphere through evaporation of rain from stratiform clouds. To mimic the vertical structure of the three clouds types introduced above, we assume that the thermal forcing $\tilde{\tilde{S}}_\theta$ is based on the first two baroclinic modes in the free troposphere. Earlier examples of models with heating defined by two baroclinic modes include [10] and [3]. In addition, the figure 3 in [19] indicates that the principle component time series of the two leading empirical orthogonal functions have dominant diurnal periodicity in sinusoidal variation. In general, we can prescribe this heating forcing as follows

$$\tilde{\tilde{S}}_\theta = H_1(y)\sin(kX+\omega t)(-\sin(z)) + \alpha H_2(y)\sin(kX+\omega t+\beta)(-2\sin(2z)) \tag{18}$$

where both $H_1(y)$ and $H_2(y)$ only depend on y and are used to represent the meridional profile of the heating. The diurnal cycle frequency ω is 2π in units of day^{-1} and the wavenumber κ is $\pi/20$ in units of $10^{-3}km^{-1}$. Two specific examples are examined in the following subsections.

3.1 A simple heating profile in the first two baroclinic modes

The three cloud types(congestus, deep convective, stratiform) and their life cycle have been investigated through observations of organized tropical convection [14,26]. In this cloud life cycle, congestus clouds serve to moisten and precondition the middle troposphere prior to deep convection. Deep convective clouds warm and dry the entire troposphere through large amounts of rainfall. Then stratiform clouds warm and dry the upper troposphere, cool and moisten the lower troposphere after deep convection. Using the multicloud model [16–18], Frenkel et al. [8] successfully reproduce several key features of the realistic tropical precipitation over continental regions by building simple multicloud models with the first two baroclinic modes of vertical structure in the free troposphere as well as the bulk atmospheric boundary layer dynamics. By identifying a cycle of five phases for the diurnal cycle of precipitation over land, they explained the underlying physical mechanism and dynamical behaviors in terms of the interactions of the three cloud types with the periodically forcing boundary layer dynamics. Some of the key features are as follows. In the early morning, direct solar heating produces convective activity and detrainment of shallow clouds from the boundary layer. In the late morning/early afternoon, congestus heating slightly warms the lower troposphere and cools the upper troposphere, which delays the reinitiation of deep convection. Meanwhile, the shallow cumulus entrainment and detrainment fluxes moisten the middle atmosphere and precondition deep convection. In the late afternoon, the massive amount of precipitation is released in the explosive afternoon deep convection episode, which warms the entire troposphere through latent heat. After sunset, the moisture recovers quickly and the troposphere nearly reaches a radiative-convective equilibrium (RCE) state by balancing precipitation and the imposed radiative cooling. Here we try to prescribe such thermal forcing which is qualitatively consistent with those key features.

Suppose deep convective clouds in the first baroclinic mode and congestus/stratiform clouds in the second baroclinic mode only have the first two parabolic cylinder functions as their meridional profiles, we can prescribe the heating as follows

$$\tilde{\tilde{S}}_\theta = \sin(kX+\omega t)\left[\phi_{0|1}+\gamma\phi_{1|1}\right](-\sin(z)) + \alpha\sin(kX+\omega t+\beta)\left[\phi_{0|2}+\gamma\phi_{1|2}\right](-2\sin(2z)) \tag{19}$$

where $\left\{\phi_{m|q}\right\}$ are functions of y, $m=0,1$; $q=1,2$ as shown in the left panel of Fig. 1. The relative strength of the second baroclinic mode $\alpha=\frac{1}{3}$ and the phase draft $\beta=\frac{\pi}{4}$ are two constant parameters which are used to control the spatial pattern of the heating at a specific season without the intraseasonal time scale dependence. We can change the meridional profiles $H_1=\phi_{0|1}+\gamma\phi_{1|1}$ and $H_2=\phi_{0|2}+\gamma\phi_{1|2}$ by adjusting the value of parameter γ. For simplicity, here we only choose the leading two meridional modes for each baroclinic mode to mimic different meridional profiles of the heating in different seasons. If $\gamma=0$, H_1 and H_2 are symmetric about the equator, which can be used to mimic the equinox case. If $\gamma=1$, H_1 and H_2 reach the maximum value at a positive y value in the northern hemisphere. If $\gamma=-1$,

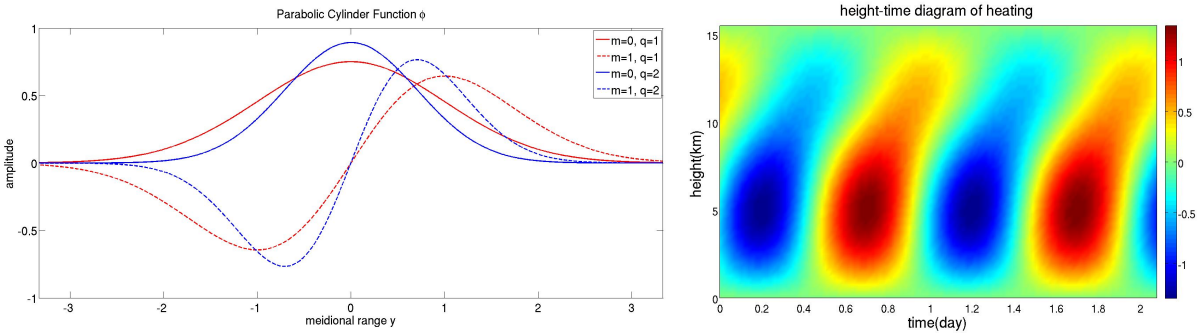

Fig. 1 The left figure shows meridional profile $\phi_{m|q}, m = 1, 2; q = 1, 2$. The right figure shows heating profile around the equator during equinox at $y = 0$ and $\gamma = 0$. Heating is in units of $4.5Kday^{-1}$.

H_1 and H_2 reach the maximum value at a negative y value in the southern hemisphere. The dynamical behavior of the heating in height is depicted in the right panel of Fig. 1, where the heating center moves from the lower troposphere to the middle troposphere and finally reaches the upper troposphere, which is consistent with the cloud life cycle from congestus clouds in the lower troposphere to deep convective clouds throughout the whole troposphere and to stratiform clouds in the upper troposphere. The curves in the left panel show different meridional profiles of heating during equinox and boreal summer, which is consistent with the observation that in annual mean ($\gamma = 0$), the heating mainly centers in the continental regime around the equator and during boreal summer ($\gamma = 1$), the heating reaches the maximum value in the continental regime of the northern hemisphere [19].

With the explicit solutions (Appendix B) for *the planetary-scale system on the daily time scale*(16a-16e), we can calculate the inertial oscillations in the diurnal cycle and the eddy flux divergences of momentum and temperature F^u, F^θ that appear in *the second-order planetary scale system on the intraseasonal time scale* (15a-15e)

$$F^u = -\frac{\partial}{\partial y}\langle \tilde{\tilde{v}}\tilde{\tilde{u}}\rangle - \frac{\partial}{\partial z}\langle \tilde{\tilde{w}}\tilde{\tilde{u}}\rangle \tag{20}$$

$$F^\theta = -\frac{\partial}{\partial y}\left\langle \tilde{\tilde{v}}\tilde{\tilde{\theta}}\right\rangle - \frac{\partial}{\partial z}\left\langle \tilde{\tilde{w}}\tilde{\tilde{\theta}}\right\rangle \tag{21}$$

Several features of these eddy flux divergences are important. First, F^u, F^θ do not depend on the daily time scale t, but they can still vary on the intraseasonal time scale T in general. Secondly, since upscale flux divergences F^u, F^θ are induced by the diurnal cycle heating in the first and second baroclinic modes, it can be shown that upscale flux divergences F^u, F^θ are in the first and third baroclinic modes (Appendix B), and the third baroclinic mode provides extensive vertical structure to capture more realistic features in reality. Thirdly, the magnitudes of F^u, F^θ are proportional to $\alpha \sin(\beta)$. If $\alpha = 0$, the heating $\tilde{\tilde{S}}_\theta$ is vertically symmetric with respect to the middle layer of the whole troposphere since there exists only the deep convective clouds in the first baroclinic mode. If $\beta = 0$, the first baroclinic mode for deep convective clouds and the second baroclinic mode for congestus/stratiform clouds are in phase. In both two cases above, F^u, F^θ are zero, meaning that there is no upscale transport of kinetic and thermal energy to the planetary/intraseasonal scales.

Now we adjust the parameter γ in the expression of $\tilde{\tilde{S}}_\theta$ to mimic the equinox case and boreal summer case, calculate the corresponding planetary-scale flow on the daily time scale, and discuss eddy flux divergences of momentum and temperature F^u, F^θ in Fig. 2.

During boreal summer, the maximum dimensionless magnitude of F^u is around 0.1 and that of F^θ is around 1, which corresponds to $0.15m/s/day$ for momentum forcing and $0.45K/day$ for thermal forcing on the planetary/intraseasonal scales. Since the thermal forcing is nondimensionalized by $0.45K/day$, there is significant eddy flux divergence of temperature. The maximum dimensionless magnitude of the thermal forcing F^θ is about 10 times that of the momentum forcing F^u. Thus the eddy flux divergence of temperature dominates. Several features of the thermal forcing F^θ are important. First, there is strong heating in the middle troposphere of the northern hemisphere and cooling in the the upper and lower troposphere of the northern hemisphere and even the whole troposphere around the equator. The maximum dimensionless magnitude of heating is three times that of cooling, which is intuitively possible because F^u, F^θ are in the first and third baroclinic modes. Secondly, although the vertical component $-\frac{\partial}{\partial z}\left\langle \tilde{\tilde{w}}\tilde{\tilde{\theta}}\right\rangle$

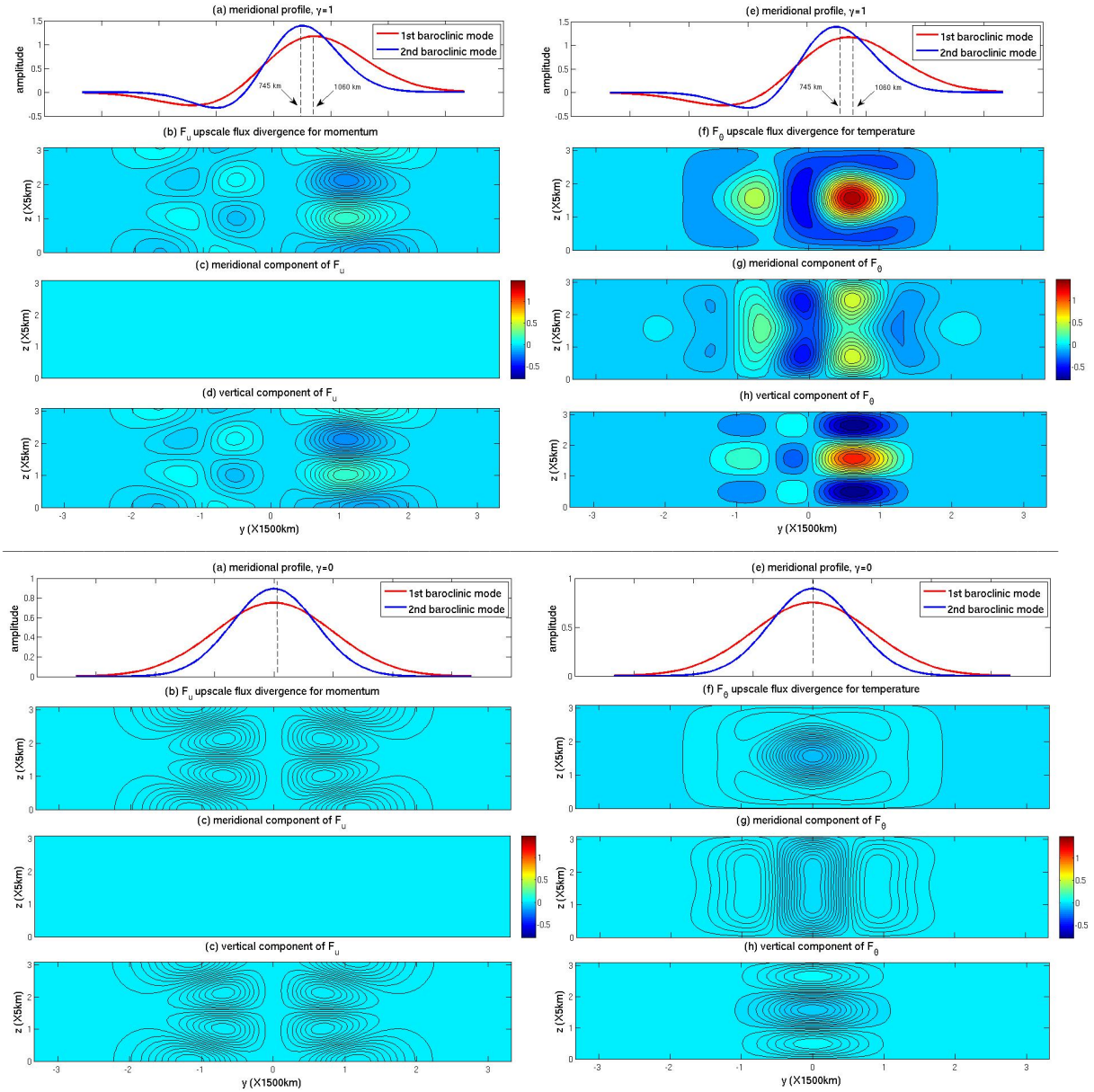

Fig. 2 The upper figure shows eddy flux divergences of momentum and temperature F^u, F^θ during boreal summer. The lower figure is for the equinox case. In each figure, the eight panels show (a) meridional profile of heating; (b) eddy flux divergence of momentum F^u; (c) its meridional component $-\frac{\partial}{\partial y}\left\langle \tilde{\bar{v}}\tilde{\bar{u}}\right\rangle$; (d) it vertical component $-\frac{\partial}{\partial z}\left\langle \tilde{\bar{w}}\tilde{\bar{u}}\right\rangle$; (e) meridional profile of heating; (f) eddy flux divergence of temperature F^θ; (g) its meridional component $-\frac{\partial}{\partial y}\left\langle \tilde{\bar{v}}\tilde{\bar{\theta}}\right\rangle$; (h) its vertical component $-\frac{\partial}{\partial z}\left\langle \tilde{\bar{w}}\tilde{\bar{\theta}}\right\rangle$. One dimensionless unit of F^u is $1m/s/day$ and that of F^θ is $0.45K/day$.

of F^θ is a little stronger than the meridional component $-\frac{\partial}{\partial y}\left\langle \tilde{\bar{v}}\tilde{\bar{\theta}}\right\rangle$, they are still comparable and form the significant thermal forcing F^θ. However, for momentum forcing F^u, its meridional component $-\frac{\partial}{\partial y}\left\langle \tilde{\bar{v}}\tilde{\bar{u}}\right\rangle$ is extremely weak and its vertical component $-\frac{\partial}{\partial z}\left\langle \tilde{\bar{w}}\tilde{\bar{u}}\right\rangle$ dominates but is still weak. Lastly, we can find the unphysical weak heating in the southern hemisphere due to the simplicity of the heating profile (19).

During equinox, both F^u, F^θ are quite weak, shown in the lower panels of Fig. 2. Thus we conclude that there is quite weak direct intraseasonal impact of the diurnal cycle during equinox, although there is also a possible indirect effect of the diurnal cycle on synoptic and mesoscale dynamics, which in turn impacts the intraseasonal scale dynamics.

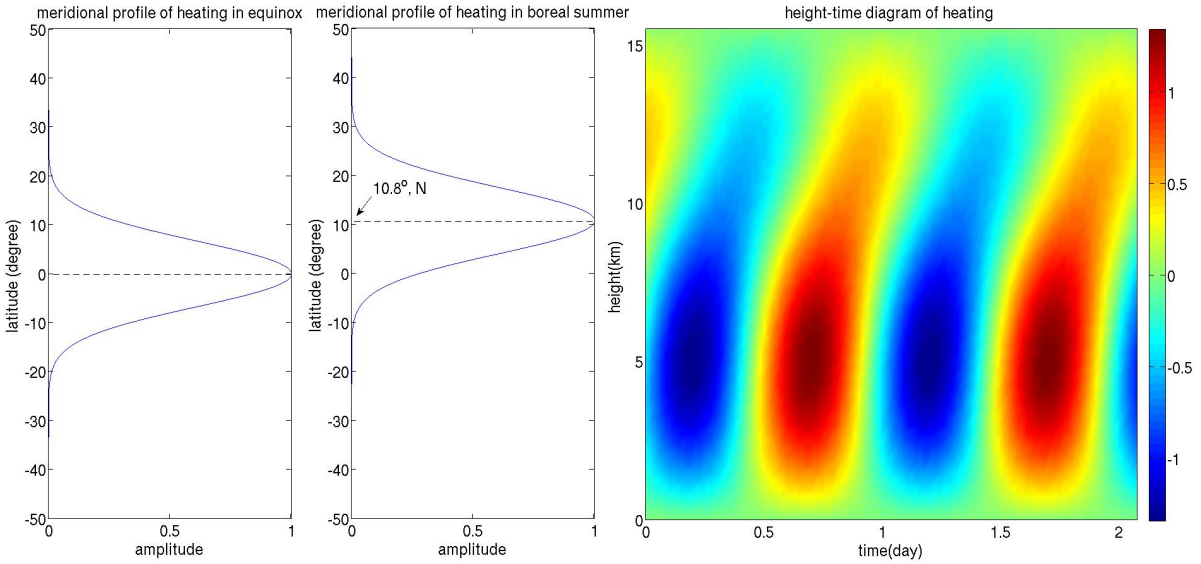

Fig. 3 The meridional profile of heating during equinox is shown in the left panel and that during boreal summer is shown in the middle panel. The meridional profile in the middle panel takes its maximum at $y = 1200km, 10.8^o N$. The right panel shows the height and time diagram of the diurnal cycle heating. Here red means heating(positive) and blue means cooling(negative). One dimensionless unit of $\tilde{\tilde{S}}_\theta$ is $4.5K/day$.

3.2 A heating profile in the first two baroclinic modes with the same meridional profile

To prescribe a more physical heating profile without loss of generality, we assume that the first baroclinic mode for deep convection clouds and the second baroclinic mode for congestus/stratiform clouds share the same meridional profile, that is $H_1(y) = H_2(y)$ in Eq. (18). In detail, the meridional profile of the diurnal cycle heating is prescribed as

$$H(y) = H_0 e^{-a(y-y_0)^2} \tag{22}$$

Fig. 3 depicts the heating profile with the meridional profile specified in Eq. (22). According to the meridional profile in Eq. (22), the diurnal cycle heating is centered at the latitude given by y_0. By varying the value of y_0, we are able to mimic different heating profiles in different seasons, as observed in [19]. During equinox, $y_0 = 0$ means that the heating reaches maximum at the equator. Here we set $a = 2, H_0 = 1$ so the strength of the heating drops to $1/e$ of its maximum magnitude around latitudes $y = \pm 1000km$, which qualitatively matches the spatial pattern of diurnal precipitation in the annual mean. During boreal summer, $y_0 = 0.8$ means $1200km$ away from the equator in the northern hemisphere. Here we set $a = 2, H_0 = 1$ so that the strength of the heating drops to $1/e$ of its maximum magnitude at latitudes $y = 2300km, y = 140km$, which also qualitatively matches the spatial pattern of diurnal precipitation during boreal summer. Since the spatial patterns of the diurnal precipitation in different seasons are different, in the following content, we will always discuss the equinox case and the boreal summer case respectively.

With the explicit solutions (Appendix B) for *the planetary-scale system on the daily time scale*(16a-16e), we can calculate the inertial oscillations in the diurnal cycle and the eddy flux divergences of momentum and temperature F^u, F^θ that appear in *the second-order planetary scale system on the intraseasonal time scale* (15a-15e)

Now we adjust the parameter y_0 in the expression of $\tilde{\tilde{S}}_\theta$ for the equinox case and boreal summer case, calculate the corresponding planetary-scale flow on the daily time scale, and discuss eddy flux divergences of momentum and temperature F^u, F^θ (20-21) in Fig. 4.

During boreal summer, the resulting eddy flux divergences of momentum and temperature share many similar properties as the case in section 3.1. The most crucial property is that the thermal forcing F^θ on the planetary/intraseasonal scales is still very strong , meaning that there is significant upscale flux feedback of temperature and the eddy flux divergence of temperature F^θ dominates. There is strong heating in the middle troposphere of the northern hemisphere and cooling surrounding the heating center and at higher latitudes of the northern hemisphere. During equinox, both F^u, F^θ are quite weak, so there is weak intraseasonal impact of the diurnal cycle during equinox.

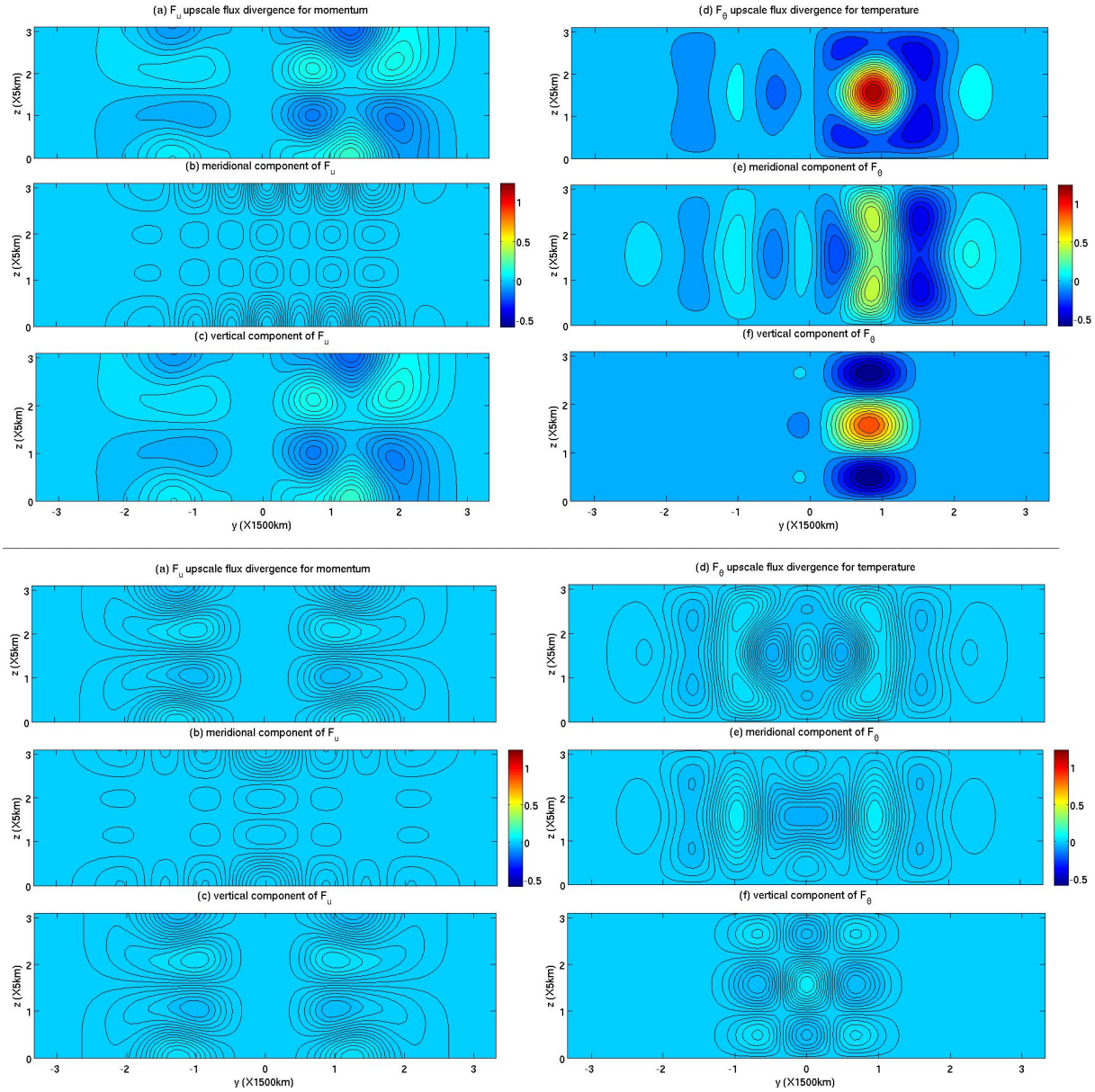

Fig. 4 The upper figure shows eddy flux divergences of momentum and temperature F^u, F^θ during boreal summer ($y_0 = 0$). The lower figure is for an equinox case ($y_0 = 0.8$). In each figure, the six panels show (a) eddy flux divergence of momentum F^u; (b) its meridional component $-\frac{\partial}{\partial y}\left\langle \tilde{\bar{v}}\tilde{\bar{u}} \right\rangle$; (c) its vertical component $-\frac{\partial}{\partial z}\left\langle \tilde{\bar{w}}\tilde{\bar{u}} \right\rangle$; (d) eddy flux divergence of temperature F^θ; (e) its meridional component $-\frac{\partial}{\partial y}\left\langle \tilde{\bar{v}}\tilde{\bar{\theta}} \right\rangle$; (f) its vertical component $-\frac{\partial}{\partial z}\left\langle \tilde{\bar{w}}\tilde{\bar{\theta}} \right\rangle$. One dimensionless unit of F^u is $1m/s/day$ and that of F^θ is $0.45K/day$.

4 The Intraseasonal Impact of the Diurnal Cycle on the Planetary Scale

In this section, the planetary-scale circulation on the intraseasonal time scale is studied. According to the multi-scale asymptotic results in section 2, there are two systems on the planetary/intraseasonal scales. The first system (Eqs. 10a-10c) deals with the winds $\langle \overline{v} \rangle, \langle \overline{w} \rangle$, which is derived from the leading-order asymptotic expansion of the primitive equations(2a-2e). Since the dimensional units of $\langle \overline{v} \rangle, \langle \overline{w} \rangle$ are $5m/s, 1.6cm/s$ separately, this system can be utilized as a model for the Hadley cell. The second system (Eqs. 15a-15e) is about $\langle \bar{u} \rangle, \langle \bar{p} \rangle, \langle \bar{\theta} \rangle, \langle \bar{v}_2 \rangle, \langle \bar{w}_2 \rangle$, which is derived from the second-order asymptotic expansion of the primitive equations (2a-2e). The dimensional units of $\langle \overline{v}_2 \rangle, \langle \overline{w}_2 \rangle$ are $0.5m/s, 0.16cm/s$ separately, thus $\langle \overline{v}_2 \rangle, \langle \overline{w}_2 \rangle$ can be understood as the circulation anomalies on the planetary/intraseasonal scales induced by the diurnal cycle heating driving eddy flux divergences F^u, F^θ. The objective here is to understand the nature of the planetary/intraseasonal scale circulation anomalies that arise from different diurnal cycle heating patterns during equinox and boreal summer.

4.1 A Model for the Hadley cell

The Hadley circulation consists of two overturning thermally direct cells in the low latitudes of both hemispheres. Observations indicate that two Hadley cells, symmetric about the equator, are rarely observed even in the equinoctial seasons. In boreal summer or winter, the winter hemisphere branch of the Hadley cell is much stronger than the summer hemisphere branch [12]. In fact, Eqs. (23a-23c) are derived from the leading-order asymptotic expansion of the primitive equations (2a-2e), and $\langle \bar{v} \rangle, \langle \bar{w} \rangle, \langle \bar{S}_u \rangle, \langle \bar{S}_\theta \rangle$ are on the planetary/intraseasonal scales. The dimensional units of $\langle \bar{S}_u \rangle, \langle \bar{S}_\theta \rangle$ are $15m/s/day, 4.5K/day$ separately, and the dimensional units of $\langle \bar{v} \rangle, \langle \bar{w} \rangle$ are $5m/s, 1.6cm/s$ separately. Here we assume the buoyancy frequency N^2 and the density ρ to be constant.

$$-y \langle \bar{v} \rangle = \langle \bar{S}_u \rangle \tag{23a}$$

$$N^2 \langle \bar{w} \rangle = \langle \bar{S}_\theta \rangle \tag{23b}$$

$$(\langle \bar{v} \rangle)_y + \langle \bar{w} \rangle_z = 0 \tag{23c}$$

Considering that Eqs. (23a-23c) describe the leading-order planetary scale flow on the intraseasonal time scale, we can use them to model the Hadley cell. Since the meridional velocity $\langle \bar{v} \rangle$ is directly determined by the momentum forcing $\langle \bar{S}_u \rangle$ and the vertical velocity $\langle \bar{w} \rangle$ is determined by the heating $\langle \bar{S}_\theta \rangle$, there is a careful balance between the momentum forcing $\langle \bar{S}_u \rangle$ and the heating $\langle \bar{S}_\theta \rangle$ if we combine Eqs. (23a,23b) with the incompressibility condition (23c)

$$\left(\frac{\langle \bar{S}_u \rangle}{y} \right)_y = \left(\frac{\langle \bar{S}_\theta \rangle}{N^2} \right)_z \tag{24}$$

The system (23a-23c) is independent of other systems and only forced by the leading-order zonal momentum forcing and thermal forcing on the planetary/intraseasonal scales. Unless $\langle \bar{S}_u \rangle, \langle \bar{S}_\theta \rangle$ satisfy the constraint (24), these equations can not be solved. In general, we can prescribe arbitrary $\langle \bar{S}_u \rangle, \langle \bar{S}_\theta \rangle$ satisfying the constraint(24) and get the corresponding leading-order planetary/intraseasonal scale circulation. Here we prescribe the momentum forcing $\langle \bar{S}_u \rangle$ and thermal forcing $\langle \bar{S}_\theta \rangle$ to qualitatively match the key features of the Hadley cell.

During equinox, the Hadley cell is symmetric about the equator. For each cell, there is rising motion near the equator, poleward flow in the upper troposphere, descending motion in the subtropics, and equatorward flow near the surface. The heating and zonal momentum forcing are specified in Eq. (25). The spatial patterns of the forcings and the resulting meridional and vertical flow field are shown in the upper panels of Fig. 5.

$$S_\theta = \left(1 - y^2\right) e^{-y^2/2} \sin(z)\,;\; S_u = y \int_{-\infty}^{y} \left(1 - s^2\right) e^{-s^2/2} ds \, \cos(z) \tag{25}$$

.

During boreal summer, the winter hemisphere branch of the Hadley cell is much stronger than the summer hemisphere branch. The heating and zonal momentum forcing are specified in Eq. (26). The spatial patterns of the forcings and the resulting meridional and vertical flow field are shown in the lower panels of Fig. 5.

$$S_\theta = \left[y e^{-y^2} - 0.2\,(y-2)\, e^{-2(y-2)^2} \right] \sin(z)\,;\; S_u = y \int_{-\infty}^{y} \left[s e^{-s^2} - 0.2\,(s-2)\, e^{-2(s-2)^2} \right] ds \, \cos(z) \tag{26}$$

4.2 A simplified version of the intraseasonal impact of the diurnal cycle

The second-order planetary scale system (15a-15e) on the intraseasonal time scale describes the planetary/intraseasonal scale dynamic response to the diurnal cycle of tropical convection. It is derived from the second-order asymptotic expansion of the primitive equations (2a-2e). There are two pieces of eddy flux divergences of momentum in the zonal momentum equation and two pieces of eddy flux divergences of temperature in the thermal equation. In each equation, the first piece corresponds to upscale feedback from the synoptic scale to the planetary scale, which has been utilized to successfully generate key

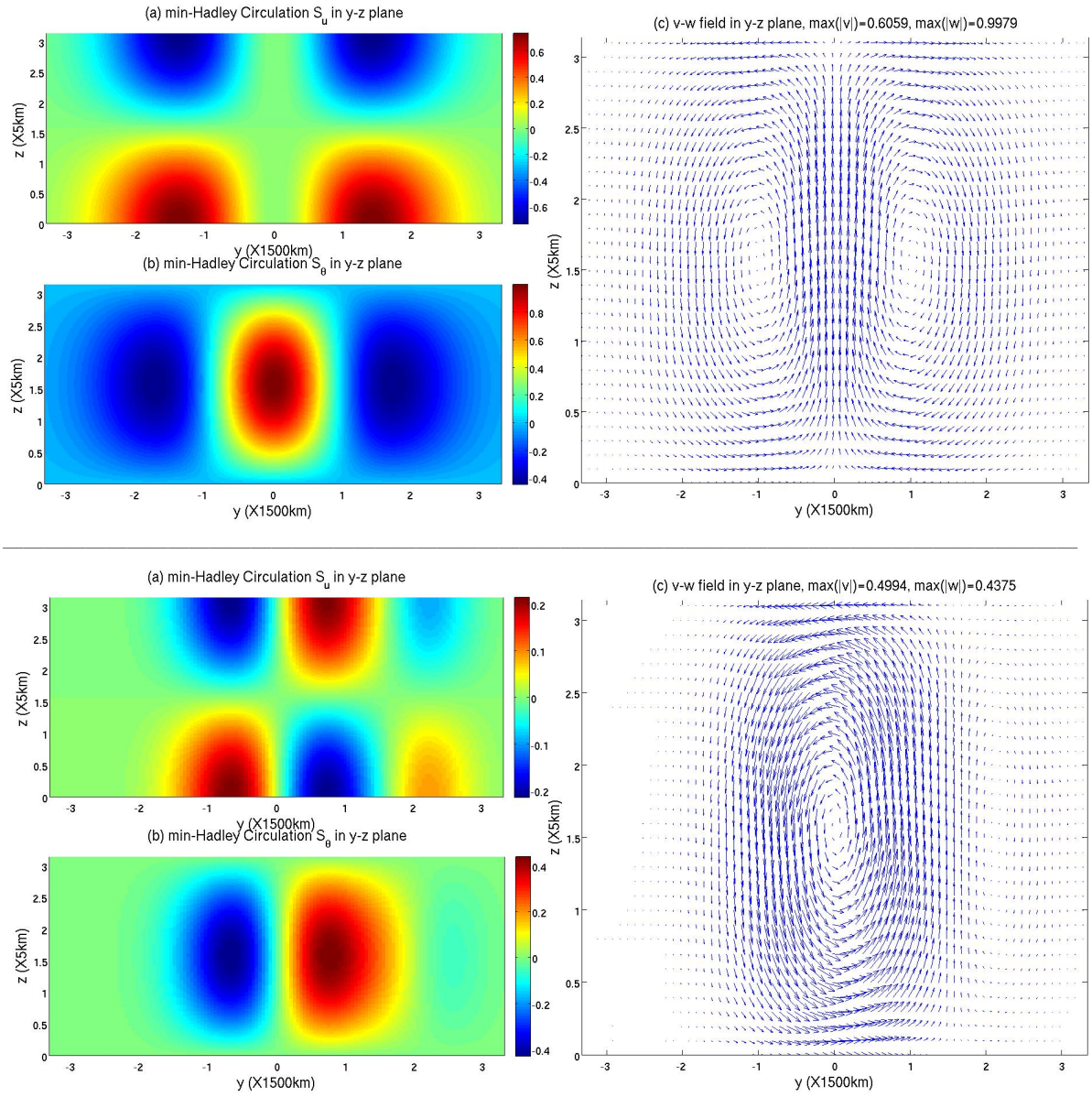

Fig. 5 The upper three panels shows the equinox case. The lower three panels are the boreal summer case. (a) zonal momentum forcing; (b) thermal forcing; (c) meridional and vertical flow field. For zonal momentum forcing, blue means westward and red means eastward. For thermal forcing, blue means cooling and red means heating. The units of $\langle \bar{S}_u \rangle, \langle \bar{S}_\theta \rangle, \langle \bar{v} \rangle, \langle \bar{w} \rangle$ are $15m/s/day$, $4.5K/day$, $5m/s$ and $1.6cm/s$ respectively.

features of MJO [24,3,4]. The second piece corresponds to upscale feedback from the daily time scale to the intraseasonal time scale. In order to consider the intraseasonal impact of the diurnal cycle in a simplified case, we consider the zonally symmetric version of the second-order planetary scale system (Eqs. 15a-15e), neglect the upscale feedback across multiple spatial scales and just focus on the upscale feedback across multiple temporal scales. All synoptic-scale variables $(u', v', p', \theta', w')$ are set to zero. Also, we assume that there is no extra momentum forcing $\langle \bar{S}_{u,2} \rangle$, $\langle \bar{S}_{v,1} \rangle$ and thermal forcing $\langle \bar{S}_{\theta,2} \rangle$ on the planetary/intraseasonal scales. To consider a simplified version, we assume that there is no leading-order planetary/intraseasonal scale circulation in section (4.1), which means there is no advection effects in the system (15a-15e) . Lastly, we assume that the buoyancy frequency N^2 and the density ρ are constants. To be brief, we rename all physical variables $u = \langle \bar{u} \rangle, p = \langle \bar{p} \rangle, \theta = \langle \bar{\theta} \rangle, v = \langle \bar{v}_2 \rangle, w = \langle \bar{w}_2 \rangle$, and we can obtain a simplified version of the second-order planetary scale system on the intraseasonal time scale

$$\frac{\partial}{\partial T} u - yv = -du + F^u \tag{27a}$$

$$yu = -p_y \tag{27b}$$

$$\frac{\partial}{\partial T}\theta + w = -d_\theta \theta + F^\theta \tag{27c}$$

$$p_z = \theta \tag{27d}$$

$$v_y + w_z = 0 \tag{27e}$$

We assume rigid lid boundary conditions at top and bottom of the troposphere,

$$w\left(X, T, y, z\right)|_{z=0,\pi} = 0 \tag{28}$$

where in dimensionless unit $z = 0$ represents the surface of the earth and $z = \pi$ represents the top of the troposphere. The momentum damping coefficient d is $1/5day^{-1}$ and the temperature damping coefficient d_θ is $1/15day^{-1}$. F^u, F^θ represent upscale feedback from the daily scale to the intraseasonal time scale in the zonal momentum equation and the thermal equation respectively

$$F^u = -\frac{\partial}{\partial y}\left\langle \tilde{\tilde{v}}\tilde{\tilde{u}}\right\rangle - \frac{\partial}{\partial z}\left\langle \tilde{\tilde{w}}\tilde{\tilde{u}}\right\rangle; F^\theta = -\frac{\partial}{\partial y}\left\langle \tilde{\tilde{v}}\tilde{\tilde{\theta}}\right\rangle - \frac{\partial}{\partial z}\left\langle \tilde{\tilde{w}}\tilde{\tilde{\theta}}\right\rangle \tag{29}$$

This system is driven by eddy flux divergences of momentum and temperature F^u, F^θ, which are associated with the planetary-scale flow on the daily time scale (16a-16e). The physical variables in this system consist of the leading-order physical variables u, p, θ and the second-order physical variables v, w. The second-order meridional velocity v and vertical velocity w can be understood as the planetary-scale circulation anomalies induced by the intraseasonal impact of the diurnal cycle of tropical convection. In the following discussion, we consider the different behavior of the planetary/intraseasonal scale dynamics in Eqs. (27a-27e,28) during equinox and boreal summer in an ideal zonally symmetric case.

In order to analyze the intraseasonal impact of the diurnal cycle of tropical convection, we plot and discuss the planetary/intraseasonal scale steady state circulation corresponding to eddy flux divergences F^u, F^θ. The forcings F^u, F^θ can be evaluated explicitly through Eq. (29) [see Appendix B] and the planetary/intraseasonal scale equations (27a-27e) can be solved by spectral expansion techniques [22]. The numerical method used here follows [4].

Since two cases of diurnal cycle heating have been prescribed in section 3, here we first consider the case with a simple heating profile utilizing the first two baroclinic modes in section 3.1. The corresponding eddy flux divergences of momentum and temperature F^u, F^θ shown in Fig. 2 are imposed into Eqs. (27a-27e). Fig. 6 shows all physical variables in the meridional and vertical directions, including pressure p, potential temperature θ as well as velocity components u, v, w.

During boreal summer, the dimensionless maximum magnitudes of all physical variables are larger than 0.1 and that of potential temperature θ even reaches 1, which is intuitively consistent with the significant eddy flux divergence of temperature F^θ shown in Figure 2. There are several crucial features of the resulting planetary/intraseasonal scale circulation. First, for the meridional and vertical flow field, a circulation cell forms around the equator, which is characterized by ascent in the northern hemisphere, southward motion in the upper troposphere, descent around the equator and northward motion in the lower troposphere. Secondly, the intraseasonal impact of the diurnal cycle on the planetary scale includes negative potential temperature anomalies in the lower troposphere. In a moist environment, negative potential temperature anomalies in the lower troposphere can increase the convective available potential energy(CAPE) and reduce the convective inhibition(CIN), which enhances the buoyancy of parcels in the free troposphere and provides a favorable condition for tropical convection; also, the lower temperatures reduce the saturation value of water vapor and promote more convection. Thirdly, there are several zonal jets at different height and latitudes, providing more possible features of the planetary-scale circulation.

During equinox, the planetary/intraseasonal scale circulation response is very weak and much less than 1, which is consistent with the weak eddy flux divergences F^u, F^θ shown in Fig. 2. Therefore, we can conclude that there is weak planetary/intraseasonal scale direct circulation response due to the diurnal cycle during equinox.

Now we consider the heating profile with the first two baroclinic modes sharing the same meridional profile, which is prescribed in section 3.2. Basically, during boreal summer, pressure p, potential temperature θ and zonal velocity u have the similar spatial patterns and magnitudes as the case we discuss above. As for the meridional and vertical flow field, a circulation cell still forms around the equator. Besides, there are two weak circulation cells in the upper and lower troposphere around the equator and a strong downdraft at the higher latitude in the northern hemisphere, providing more possible features of the planetary-scale circulation. The results are shown in lower panels of Fig. 6.

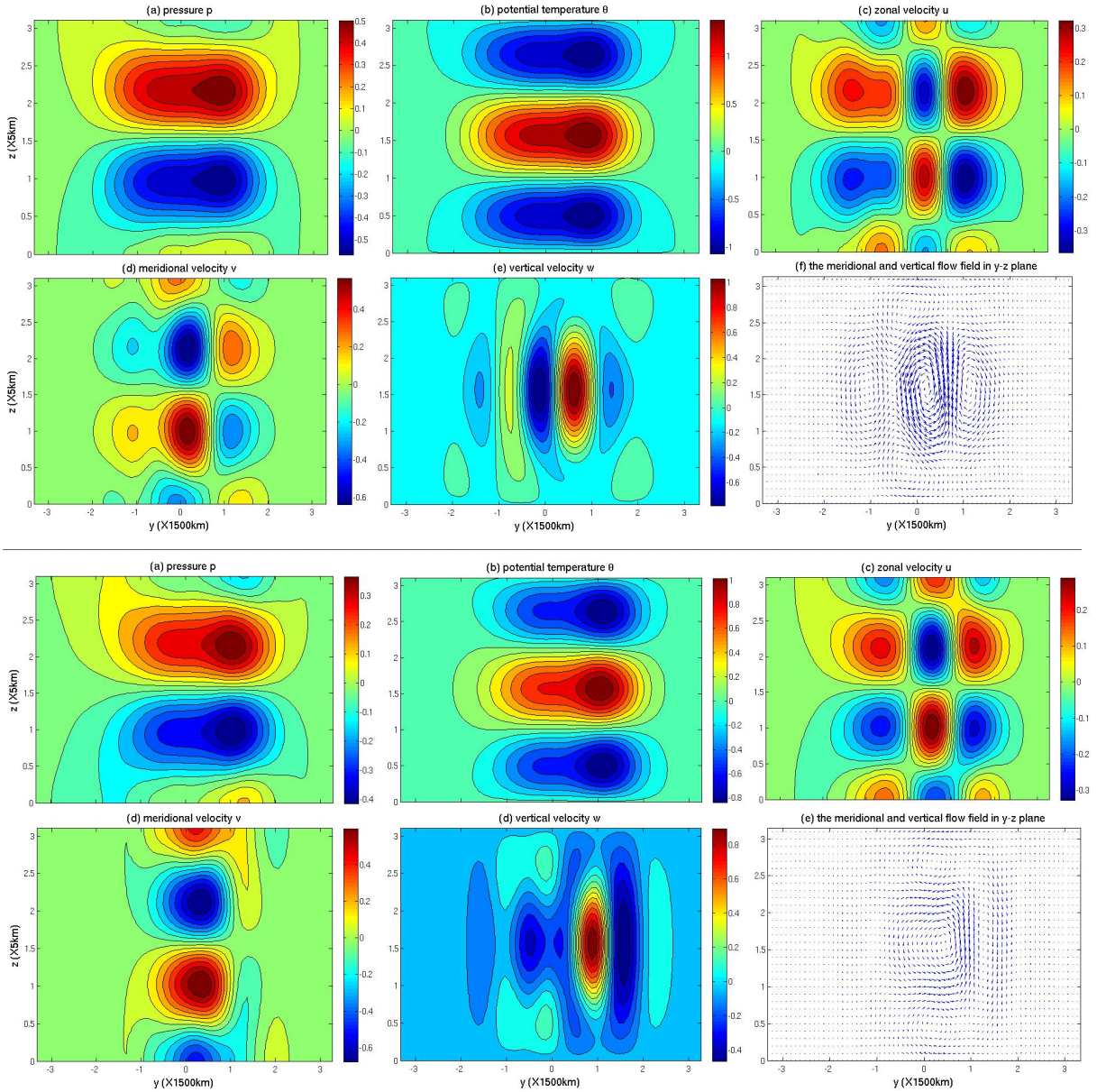

Fig. 6 The upper figure shows the large-scale flows induced by upscale flux divergences F^u, F^θ during boreal summer corresponding to the heating in section 3.1. The lower figure shows the case corresponding to the heating in section 3.2. (a) pressure p; (b) potential temperature θ; (c) zonal velocity u; (d) meridional velocity v; (e) vertical velocity w; (f) the meridional and vertical flow field. The units of p, θ, u, v, w are $250m^2/s^2$, $1.5K$, $5m/s$, $0.5m/s$, $5m/s$, $0.16cm/s$ respectively.

4.3 A fully coupled version of the intraseasonal impact of the diurnal cycle on the Hadley cell

In section (4.2), we neglect the advection effects of the leading-order meridional and vertical flow field from the model for the Hadley cell (23a-23c) . Such a simplified version of the planetary/intraseasonal scale circulation response can shed some light on the intraseasonal impact of the diurnal cycle through Eqs. (27a-27e). As demonstrated in section 4.1 and Fig. 5, the system (23a-23c) on the planetary/intraseasonal scales is capable of mimicking a Hadley cell by creating two circulation cells with the symmetric spatial pattern during equinox and an asymmetric spatial pattern during boreal summer. Therefore, a fully coupled version of the multi-scale model involving the Hadley cell can be utilized to model more realistic atmospheric dynamics in the tropics for the intraseasonal impact of the diurnal cycle. In this section, we add the mean flow from the model of the Hadley cell (23a-23c) and consider how such advection effect from the mean flow can affect the second-order planetary scale system on the intraseasonal time scale (15a-15e). Here we still consider an ideal zonally symmetric case. All synoptic-scale variables $(u', v', p', \theta', w')$ are set to zero. There is no extra momentum forcing $\langle \bar{S}_{u,2} \rangle$, $\langle \bar{S}_{v,1} \rangle$ and thermal forcing $\langle \bar{S}_{\theta,2} \rangle$ on the planetary/intraseasonal scales. Also, we assume that the buoyancy frequency N^2 and the density ρ are

constants. To be brief, we rename all physical variables $u = \langle \bar{u} \rangle, p = \langle \bar{p} \rangle, \theta = \langle \bar{\theta} \rangle, v = \langle \bar{v}_2 \rangle, w = \langle \bar{w}_2 \rangle$ and the Hadley cell flow field $V = \langle \bar{v} \rangle, W = \langle \bar{w} \rangle$, and obtain a fully coupled version of the second-order planetary scale system on the intraseasonal time scale.

$$\frac{\partial}{\partial T}u + V\frac{\partial}{\partial y}u + W\frac{\partial}{\partial z}u - yv = -du + F^u \tag{30a}$$

$$yu = -p_y \tag{30b}$$

$$\frac{\partial}{\partial T}\theta + V\frac{\partial}{\partial y}\theta + W\frac{\partial}{\partial z}\theta + w = -d_\theta\theta + F^\theta \tag{30c}$$

$$p_z = \theta \tag{30d}$$

$$v_y + w_z = 0 \tag{30e}$$

We assume rigid lid boundary conditions at top and bottom of the troposphere,

$$w\left(X, T, y, z\right)|_{z=0,\pi} = 0 \tag{31}$$

where in dimensionless unit $z = 0$ represents the surface of the earth and $z = \pi$ represents the top of the troposphere. This system is advected by the meridional and vertical velocity components V, W from the model for the Hadley cell (23a-23c). F^u, F^θ (29) represent upscale feedback from the daily scale to the intraseasonal time scale in the zonal momentum equation and the thermal equation respectively.

Since the intraseasonal impact of the diurnal cycle of tropical convection during boreal summer is much stronger than that during equinox, hereafter we only show the planetary/intraseasonal scale circulation response to the eddy flux divergences F^u, F^θ during boreal summer. The eddy flux divergences of momentum and temperature F^u, F^θ can be evaluated explicitly through Eq. (29) (see Appendix B). The only difference between the fully coupled version (Eqs. 30a-30e) and the simplified version (Eqs. 27a-27e) is that in this case there are advection effects from the model for the Hadley cell in Eqs. (30a-30e). The planetary/intraseasonal scale equations (30a-30e) can still be solved numerically by spectral expansion techniques [22] and the Galerkin method. The basic idea behind the numerical method is that since the Hadley cell is in the first baroclinic mode, all the vertical modes in the solutions are coupled with each other due to the advection effects. For each baroclinic mode, we use the Galerkin method and make sure all equations are held for a finite set of basis functions. Instead of solving the problem in each single baroclinic mode, we need to solve the problem by coupling all the vertical modes together, including the baroclinic modes and the barotropic mode. The details for the numerical method can be found at Appendix C.

Since two kinds of diurnal cycle heating have been prescribed in section 3, we first consider the case with a simple heating profile in the first two baroclinic modes as described in section 3.1. The corresponding eddy flux divergences of momentum and temperature F^u, F^θ shown in Fig. 2 are imposed into Eqs. (30a-30e). The upper panels of Fig. 7 show all physical variables in the meridional and vertical directions, including pressure p, potential temperature θ, velocity components u, v, w as well as the meridional and vertical components of the velocity field from sec. 4.1 and the modified Hadley cell.

There are several new features arising when we couple the model for the Hadley cell with the planetary/intraseasonal scale circulation anomalies induced by the model of the diurnal cycle. First, the maximum magnitude of the pressure p and the potential temperature θ decreases, compared with the simple version shown in Fig. 6. Due to the advection effects of the Hadley cell, the spatial patterns of the pressure p and the potential temperature θ become meridionally tilted. Secondly, the maximum magnitude of the zonal velocity u increases and the spatial pattern of the zonal jets also changes, compared with the simple case without advection effects in Fig. 6. In the present case, strong westerly winds form in the middle troposphere of the northern hemisphere and strong easterly winds form in the middle troposphere of the southern hemisphere. Thirdly, there exists a circulation cell at the upper troposphere around the equator. According to the panels $(g), (h)$ of Fig. 7, we can find that such a circulation cell can strengthen the upper branch of the winter cell of the Hadley circulation, since this circulation cell moves in the same direction of the Hadley cell. Also, there exists another circulation cell in the lower troposphere around the equator. This circulation cell moves in the opposite direction of the Hadley cell, thus it can weaken the lower branch of the winter cell of the Hadley circulation. Finally, there are strong northward winds in the middle troposphere around the equator where the center of the winter cell of the Hadley circulation is located.

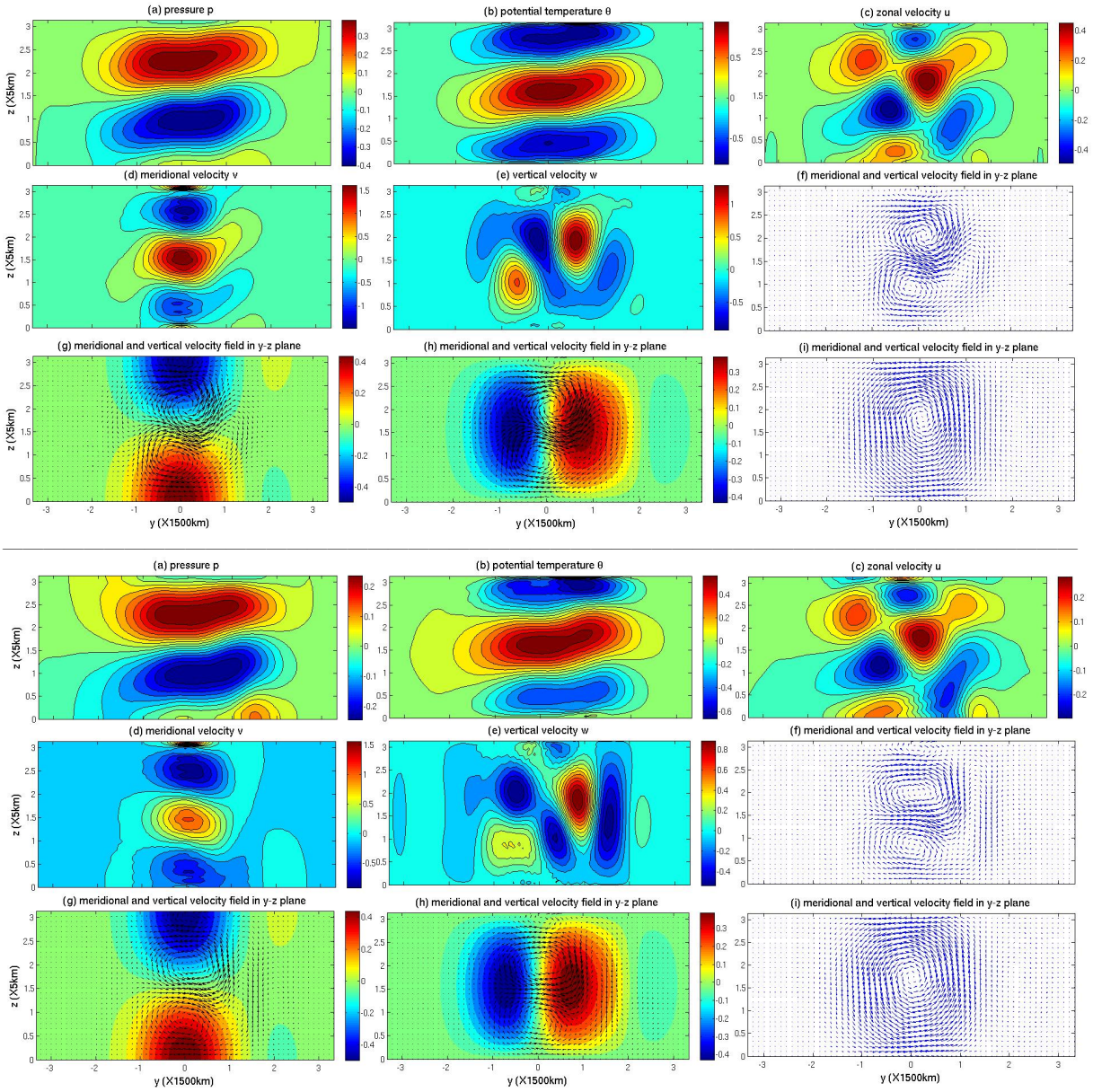

Fig. 7 The upper figure shows the large-scale flows corresponding to the heating in section 3.1. The lower figure shows the case corresponding to the heating in section 3.2. (a) pressure p; (b) potential temperature θ; (c) zonal velocity u; (d) meridional velocity v; (e) vertical velocity w; (f) the meridional and vertical flow field (v, w); (g) color means the meridional velocity of the original Hadley cell, vectors show the flow field in (f); (h) color means the vertical velocity of the original Hadley cell, vectors show the flow field in (f); (i) the modified Hadley cell, $(V + \epsilon v, W + \epsilon w)$. The units of p, θ, u, v, w are $250m^2/s^2$, $1.5K$, $5m/s$, $0.5m/s$, $5m/s$, $0.16cm/s$ and the units of V, W in the Hadley cell are $5m/s, 1.6cm/s$.

Now we consider the heating profile with the first two baroclinic modes sharing the same meridional profile as prescribed in section 3.2. The lower panels of Fig. 7 show all physical variables in the meridional and vertical directions, including pressure p, potential temperature θ, velocity components u, v, w as well as the original and modified Hadley cell. Compared with the simple case shown in Fig. 6, we can confirm the advection effects of the Hadley cell through the meridionally tilted spatial patterns of the pressure p and the potential temperature θ. The spatial patterns of the velocity components u, v, w share many similar features with the case we discuss above.

5 Concluding Discussion

In the present article, we have derived a multi-scale model by starting from the hydrostatic, anelastic Euler equations on an equatorial β-plane and following the derivation of systematic multi-scale models for tropical convection [23]. Inspired by the observation of the diurnal variability of tropical precipitation

[19], we try to assess the intraseasonal impact of planetary-scale inertial oscillations in the diurnal cycle. The appeal of this analytic multi-scale model is that it provides assessment of eddy flux divergences of momentum and temperature and their intraseasonal impact on the planetary-scale circulation in a transparent fashion. Thanks to the multi-scale asymptotics and several essential assumptions, this multi-scale model is capable of reproducing the Hadley cell and its advective effects on the planetary/intraseasonal scale circulation anomalies, allowing us to study large-scale flows in a more general framework. To assess the intraseasonal impact of the diurnal cycle of tropical precipitation on the planetary-scale flow such as the Hadley cell, four systems involving physical variables on different spatiotemporal scales have been separated from the primitive equations by using multi-scale asymptotics. In order to assess the upscale feedback from the daily time scale to the intraseasonal time scale, one system involving physical variables on the planetary scale and daily time scale has been utilized as the model for the diurnal cycle. Since the eddy flux divergences of momentum and temperature involve the planetary-scale flows on the daily time scale from the model for the diurnal cycle, the planetary/intraseasonal scale circulation forced by those eddy flux divergences can be interpreted as the intraseasonal impact of the diurnal cycle.

The model for the diurnal cycle is a linear system with all physical variables on the planetary scale and daily time scale, since the original equations are assumed to be weakly advected and all the resulting equations in the model for the diurnal cycle come from the leading-order asymptotic expansion of the primitive equations. To mimic the latent heat release associated with the diurnal cycle of tropical convection, the model utilizes three cloud types (congestus, deep convective, and stratiform) of organized tropical convection in the free troposphere [7–9]. For the eddy flux divergences of momentum and temperature, there are explicit formulas calculated by using spectral expansion techniques [22]. The results show that the eddy flux divergence of temperature during boreal summer is much stronger than that during equinox, which suggests that the significant intraseasonal impact of the diurnal cycle is traced to the meridional asymmetry of the diurnal cycle heating profile in the first two baroclinic modes. During boreal summer, the eddy flux divergence of temperature dominates in the northern hemisphere, providing a significant heating in the middle troposphere of the northern hemisphere with large-scale ascent and cooling surrounding this heating center with large-scale subsidence.

Having recognized the spatial patterns of eddy flux divergences of momentum and temperature during equinox and boreal summer, we can calculate the resulting planetary-scale circulation response on the intraseasonal time scale, which comes from the second-order asymptotic expansion of the primitive equations and indicates the upscale feedback of the diurnal cycle. In an ideal zonally symmetric case, the resulting steady state circulation on the planetary/intraseasonal scales during boreal summer is characterized by ascent in the northern hemisphere, southward motion in the upper troposphere, descent around the equator and northward motion in the lower troposphere. Also, the intraseasonal impact of the diurnal cycle on the planetary scale includes negative potential temperature anomalies in the lower troposphere, which suggests convective triggering in the tropics. The leading-order planetary/intraseasonal scale circulation is utilized as the model for the Hadley cell. Since the planetary/intraseasonal scale circulation system is advected by the Hadley cell, we are able to obtain a fully coupled version of the intraseasonal impact of the diurnal cycle on the Hadley cell. By studying such a fully coupled model, we conclude that the intraseasonal impact of the diurnal cycle can strengthen the upper branch of the winter cell of the Hadley circulation but weaken the lower branch of the winter cell of the Hadley circulation. Meanwhile, there exist strong northward winds in the middle troposphere around the equator, providing extensive features of the intraseasonal impact of the diurnal cycle on the Hadley cell.

The appeal of the multi-scale model developed in this article is that there exist explicit formulas for the eddy flux divergences of momentum and temperature for the upscale feedback across multiple spatiotemporal scales, which provides assessment of the intraseasonal impact of the diurnal cycle in a transparent fashion. In fact, the IPESD model [24,23,3,4] considers the upscale feedback from the synoptic scale to the planetary scale and successfully generates a planetary-scale circulation resembling the tropical intraseasonal oscillation. In contrast, here we consider the upscale feedback from the daily time scale to the intraseasonal time scale and explore the intraseasonal impact of the diurnal cycle. When it is coupled with the model for the Hadley cell, the multi-scale model developed here provides a clear framework for the modulation and rectification of the Hadley circulation. The framework developed here for the intraseasonal impact of the diurnal cycle may provide insight into the explanation of some tropical phenomena. One promising application of the intraseasonal impact of the diurnal cycle is to better represent the intraseasonal variability in the tropics such as Madden-Julian oscillation (MJO). It may be interesting to include the nonlinear effects of moisture across multiple spatiotemporal scales, as for example in [5], allowing this multi-scale model to generate more realistic features of tropical phenomena.

This study has some implications for comprehensive numerical models. First, according to the results in sec. 4.2 and 4.3, it can be concluded that the diurnal cycle of tropical convection during boreal summer can induce significant intraseasonal impact on the planetary scale in the tropics. Thus one of the implications of this simple asymptotic model to the comprehensive models is that it emphasizes the significance of the representation of the diurnal variability of tropical precipitation. Specifically, the heating profile utilizing three cloud types (congestus, deep convective and stratiform) on the first two barolinic modes is a good candidate [16–18]. Secondly, the eddy flux divergences of the momentum and temperature not only allow us to analytically assess the upscale effects from the daily time scale, but also provide the comprehensive numerical models with better intuition for the parameterization associated with the diurnal cycle and its intraseasonal impact. Thirdly, the planetary-scale response to the intraseasonal impact of the diurnal cycle in this model, including the lower level potential temperature anomalies, the multiple zonal jets and the overturning circulation cells, may provide theoretical predictions and physical mechanisms to improve the simulation of the flow field over the Maritime Continent in the comprehensive numerical models.

Acknowledgements This research of A.J.M is partially supported by the office of NAVAL Research ONR MURI N00014-12-1-0912 and Q.Y is supported as a graduate research assistant on this grant.

Appendices

A Details for the derivation of the multi-scale model

We start from the hydrostatic, anelastic Euler equations on an equatorial β-plane**,** Eqs. (2a-2e)

$$u_t + uu_x + vu_y + wu_z - yv = -p_x - \epsilon du + S_u \tag{32a}$$

$$v_t + uv_x + vv_y + wv_z + yu = -p_y - \epsilon dv + S_v \tag{32b}$$

$$\theta_t + u\theta_x + v\theta_y + w\theta_z + N^2 w = -\epsilon d_\theta \theta + S_\theta \tag{32c}$$

$$p_z = \theta \tag{32d}$$

$$(\rho u)_x + (\rho v)_y + (\rho w)_z = 0 \tag{32e}$$

where $\rho = \rho(z)$and $N^2 = N^2(z)$ only depend on height.

By assuming multi-scale solutions as the expression (Eq. 3), the zonal and time derivatives of an arbitrary function f^ϵ are given by chain rule

$$\frac{\partial f^\epsilon}{\partial x} + \epsilon \frac{\partial f^\epsilon}{\partial X},\ \frac{\partial f^\epsilon}{\partial t} + \epsilon \frac{\partial f^\epsilon}{\partial T} \tag{33}$$

Meanwhile, we use the ansatz(7)

$$g = \epsilon \left[g'(x, X, t, T, y, z) + \bar{g}(X, t, T, y, z) \right] + \epsilon^2 g_2,\ g \in \{u, v, w, \theta, p, S_u, S_v, S_\theta\} \tag{34}$$

We plug the ansatz into Eqs. (32a-32e), and collect all terms at the leading order.

For $\mathcal{O}(\epsilon)$:

$$\frac{\partial}{\partial t}\left(\overline{u} + u'\right) - y\left(\overline{v} + v'\right) = -\frac{\partial}{\partial x} p' + S'_u + \bar{S}_u \tag{35a}$$

$$\frac{\partial}{\partial t}\left(\overline{v} + v'\right) + y\left(\overline{u} + u'\right) = -\frac{\partial}{\partial y}\left(\bar{p} + p'\right) + S'_v + \bar{S}_v \tag{35b}$$

$$\frac{\partial}{\partial t}\left(\overline{\theta} + \theta'\right) + N^2\left(\overline{w} + w'\right) = S'_\theta + \bar{S}_\theta \tag{35c}$$

$$\frac{\partial}{\partial z}\left(\bar{p} + p'\right) = \bar{\theta} + \theta' \tag{35d}$$

$$\frac{\partial}{\partial x} u' + \frac{\partial}{\partial y}\left(\overline{v} + v'\right) + \frac{1}{\rho}\frac{\partial}{\partial z}\left(\rho\left(\overline{w} + w'\right)\right) = 0 \tag{35e}$$

By doing zonal averaging on Eqs. (35a-35e), we can get *the planetary-scale system*

$$\frac{\partial}{\partial t}\overline{u} - y\overline{v} = \bar{S}_u \tag{36a}$$

$$\frac{\partial}{\partial t}\overline{v} + y\overline{u} = -\frac{\partial}{\partial y}\bar{p} + \bar{S}_v \tag{36b}$$

$$\frac{\partial}{\partial t}\bar{\theta} + N^2\overline{w} = \bar{S}_\theta \tag{36c}$$

$$\frac{\partial}{\partial z}\bar{p} = \bar{\theta} \tag{36d}$$

$$\frac{\partial}{\partial y}\overline{v} + \frac{1}{\rho}\frac{\partial}{\partial z}\left(\rho\overline{w}\right) = 0 \tag{36e}$$

By subtracting *the planetary-scale system* (36a-36e) from Eqs. (35a-35e), we derive *the synoptic-scale system*

$$\frac{\partial}{\partial t}u' - yv' = -\frac{\partial}{\partial x}p' + S'_u \tag{37a}$$

$$\frac{\partial}{\partial t}v' + yu' = -\frac{\partial}{\partial y}p' + S'_v \tag{37b}$$

$$\frac{\partial}{\partial t}\theta' + N^2 w' = S'_\theta \tag{37c}$$

$$\frac{\partial}{\partial z}p' = \theta' \tag{37d}$$

$$\frac{\partial}{\partial x}u' + \frac{\partial}{\partial y}v' + \frac{1}{\rho}\frac{\partial}{\partial z}\left(\rho w'\right) = 0 \tag{37e}$$

Since the daily time scale is the fast time scale compared with the intraseasonal time scale, we do time averaging on Eqs. (36a-36e) and all daily time scale derivatives vanish. In the end, we get *the leading-order planetary scale system on the intraseasonal time scale*

$$-y\left\langle\overline{v}\right\rangle = \left\langle\bar{S}_u\right\rangle \tag{38a}$$

$$y\left\langle\bar{u}\right\rangle = -\frac{\partial}{\partial y}\left\langle\bar{p}\right\rangle + \left\langle\bar{S}_v\right\rangle \tag{38b}$$

$$N^2\left\langle\overline{w}\right\rangle = \left\langle\bar{S}_\theta\right\rangle \tag{38c}$$

$$\frac{\partial}{\partial z}\left\langle\bar{p}\right\rangle = \left\langle\bar{\theta}\right\rangle \tag{38d}$$

$$\frac{\partial}{\partial y}\left\langle\overline{v}\right\rangle + \frac{1}{\rho}\frac{\partial}{\partial z}\left(\rho\left\langle\overline{w}\right\rangle\right) = 0 \tag{38e}$$

By combining Eqs. (38a,38c,38e), we can get a constraint as follows

$$\frac{\partial}{\partial y}\left(\frac{\left\langle\bar{S}_u\right\rangle}{y}\right) = \frac{1}{\rho}\frac{\partial}{\partial z}\left(\rho\frac{\left\langle\bar{S}_\theta\right\rangle}{N^2}\right) \tag{39}$$

For $\mathcal{O}\left(\epsilon^2\right)$, we just look at the zonal momentum equation, the thermal equation and the mass conservation equation:

$$\begin{aligned}\frac{\partial}{\partial T}\left(\overline{u}+u'\right) + \frac{\partial}{\partial t}u_2 + \left(\overline{u}+u'\right)\frac{\partial}{\partial x}\left(\overline{u}+u'\right) + \left(\overline{v}+v'\right)\frac{\partial}{\partial y}\left(\overline{u}+u'\right) + \left(\overline{w}+w'\right)\frac{\partial}{\partial z}\left(\overline{u}+u'\right) - yv_2 \\ = -\frac{\partial}{\partial x}p_2 - \frac{\partial}{\partial X}\left(\bar{p}+p'\right) - d\left(\overline{u}+u'\right) + S_{u,2}\end{aligned}$$

$$\begin{aligned}\frac{\partial}{\partial T}\left(\bar{\theta}+\theta'\right) + \frac{\partial}{\partial t}\theta_2 + \left(\overline{u}+u'\right)\frac{\partial}{\partial x}\left(\bar{\theta}+\theta'\right) + \left(\overline{v}+v'\right)\frac{\partial}{\partial y}\left(\bar{\theta}+\theta'\right) + \left(\overline{w}+w'\right)\frac{\partial}{\partial z}\left(\bar{\theta}+\theta'\right) + N^2 w_2 \\ = -d_\theta\left(\bar{\theta}+\theta'\right) + S_{\theta,2}\end{aligned}$$

$$\frac{\partial}{\partial x}u_2 + \frac{\partial}{\partial X}\left(\overline{u}+u'\right) + \frac{\partial}{\partial y}v_2 + \frac{1}{\rho}\frac{\partial}{\partial z}\left(\rho w_2\right) = 0 \tag{40}$$

In order to guarantee the validation of multi-scale asymptotics, secular growth on spatiotemporal scales can be avoid and we have $\overline{\frac{\partial}{\partial x}f} = 0, \left\langle\frac{\partial}{\partial t}f\right\rangle = 0$.

After doing zonal averaging on the equations above, we can get

$$\frac{\partial}{\partial T}\overline{u} + \frac{\partial}{\partial t}\bar{u}_2 + \overline{v'\frac{\partial}{\partial y}u'} + \bar{v}\frac{\partial}{\partial y}\bar{u} + \overline{w'\frac{\partial}{\partial z}u'} + \bar{w}\frac{\partial}{\partial z}\bar{u} - y\bar{v}_2 = -\frac{\partial}{\partial X}\bar{p} - d\overline{u} + \overline{S_{u,2}} \tag{41}$$

$$\frac{\partial}{\partial T}\bar{\theta} + \frac{\partial}{\partial t}\bar{\theta}_2 + \overline{u'\frac{\partial}{\partial x}\theta'} + \overline{v'\frac{\partial}{\partial y}\theta'} + \bar{v}\frac{\partial}{\partial y}\bar{\theta} + \overline{w'\frac{\partial}{\partial z}\theta'} + \bar{w}\frac{\partial}{\partial z}\bar{\theta} + N^2\bar{w}_2 = -d_\theta\bar{\theta} + \overline{S_{\theta,2}} \tag{42}$$

$$\frac{\partial}{\partial X}\overline{u}+\frac{\partial}{\partial y}\bar{v}_2+\frac{1}{\rho}\frac{\partial}{\partial z}\left(\rho\bar{w}_2\right)=0 \tag{43}$$

By combining the incompressibility condition (37e) for $\mathcal{O}(\epsilon)$, we have [23]

$$\overline{u'\frac{\partial}{\partial x}\left(\rho u'\right)}+\overline{u'\frac{\partial}{\partial y}\left(\rho v'\right)}+\overline{u'\frac{\partial}{\partial z}\left(\rho w'\right)}=0 \tag{44}$$

$$\overline{\theta'\frac{\partial}{\partial x}\left(\rho u'\right)}+\overline{\theta'\frac{\partial}{\partial y}\left(\rho v'\right)}+\overline{\theta'\frac{\partial}{\partial z}\left(\rho w'\right)}=0 \tag{45}$$

Similarly, if we use the incompressibility condition(38e) for $\mathcal{O}(\epsilon)$, we have [23]

$$\overline{u}\frac{\partial}{\partial y}\left(\rho\overline{v}\right)+\overline{u}\frac{\partial}{\partial z}\left(\rho\overline{w}\right)=0 \tag{46}$$

$$\overline{\theta}\frac{\partial}{\partial y}\left(\rho\overline{v}\right)+\overline{\theta}\frac{\partial}{\partial z}\left(\rho\overline{w}\right)=0 \tag{47}$$

Now we can simplify Eqs. (41-43) by using Eqs. (44, 45, 46, 47).

$$\frac{\partial}{\partial T}\overline{u}+\frac{\partial}{\partial t}\bar{u}_2-y\bar{v}_2=-\frac{\partial}{\partial X}\bar{p}-d\overline{u}-\overline{\frac{\partial}{\partial y}\left(v'u'\right)}-\overline{\frac{1}{\rho}\frac{\partial}{\partial z}\left(\rho w'u'\right)}-\frac{\partial}{\partial y}\left(\bar{v}\bar{u}\right)-\frac{1}{\rho}\frac{\partial}{\partial z}\left(\rho\bar{w}\bar{u}\right)+\overline{S_{u,2}} \tag{48}$$

$$\frac{\partial}{\partial T}\overline{\theta}+\frac{\partial}{\partial t}\bar{\theta}_2+N^2\bar{w}_2=-d_\theta\overline{\theta}-\overline{\frac{\partial}{\partial y}\left(v'\theta'\right)}-\overline{\frac{1}{\rho}\frac{\partial}{\partial z}\left(\rho w'\theta'\right)}-\frac{\partial}{\partial y}\left(\bar{v}\bar{\theta}\right)-\frac{1}{\rho}\frac{\partial}{\partial z}\left(\rho\bar{w}\bar{\theta}\right)+\overline{S_{\theta,2}} \tag{49}$$

$$\frac{\partial}{\partial X}\overline{u}+\frac{\partial}{\partial y}\bar{v}_2+\frac{1}{\rho}\frac{\partial}{\partial z}\left(\rho\bar{w}_2\right)=0 \tag{50}$$

Similarly, we do time average on the daily time scale t on Eqs. (38b, 38d, 48-50). All daily time scale derivatives vanish $\left\langle\frac{\partial}{\partial t}\bar{u}_2\right\rangle=0;\left\langle\frac{\partial}{\partial t}\bar{\theta}_2\right\rangle=0$. Also, if we separate each planetary-scale variable into an intraseasonal time scale component and a daily time scale component,

$$\bar{u}=\langle\bar{u}\rangle+\tilde{\bar{u}};\bar{v}=\langle\bar{v}\rangle+\tilde{\bar{v}};\bar{w}=\langle\bar{w}\rangle+\tilde{\bar{w}};\bar{\theta}=\left\langle\bar{\theta}\right\rangle+\tilde{\bar{\theta}} \tag{51}$$

After time averaging, the eddy flux divergences of momentum and temperature on the planetary scale can be divided into two pieces, one piece can be interpreted as advection effects from the leading-order $\langle\bar{v}\rangle,\langle\bar{w}\rangle$, and the other piece can be understood as eddy flux divergences from the daily time scale to the intraseasonal time scale

$$-\frac{\partial}{\partial y}\left\langle\bar{v}\bar{u}\right\rangle-\frac{1}{\rho}\frac{\partial}{\partial z}\left\langle\rho\bar{w}\bar{u}\right\rangle=-\frac{\partial}{\partial y}\left\langle\left(\langle\bar{v}\rangle+\tilde{\bar{v}}\right)\left(\langle\bar{u}\rangle+\tilde{\bar{u}}\right)\right\rangle-\frac{1}{\rho}\frac{\partial}{\partial z}\left\langle\rho\left(\langle\bar{w}\rangle+\tilde{\bar{w}}\right)\left(\langle\bar{u}\rangle+\tilde{\bar{u}}\right)\right\rangle \tag{52}$$

$$=-\frac{\partial}{\partial y}\left(\langle\bar{v}\rangle\langle\bar{u}\rangle\right)-\frac{1}{\rho}\frac{\partial}{\partial z}\left(\rho\langle\bar{w}\rangle\langle\bar{u}\rangle\right)-\frac{\partial}{\partial y}\left\langle\tilde{\bar{v}}\tilde{\bar{u}}\right\rangle-\frac{1}{\rho}\frac{\partial}{\partial z}\left\langle\rho\tilde{\bar{w}}\tilde{\bar{u}}\right\rangle \tag{53}$$

If we use Eq. (38e) and multiply it by $\langle\bar{u}\rangle$, we can get

$$\langle\bar{u}\rangle\frac{\partial}{\partial y}\langle\bar{v}\rangle+\frac{1}{\rho}\langle\bar{u}\rangle\frac{\partial}{\partial z}\left(\rho\langle\overline{w}\rangle\right)=0$$

Then we can find that the first two terms in the right hand of Eq. (53) can be rewritten as

$$\begin{aligned}-\frac{\partial}{\partial y}\left(\langle\bar{v}\rangle\langle\bar{u}\rangle\right)-\frac{1}{\rho}\frac{\partial}{\partial z}\left(\rho\langle\bar{w}\rangle\langle\bar{u}\rangle\right)&=-\langle\bar{u}\rangle\frac{\partial}{\partial y}\langle\bar{v}\rangle-\frac{1}{\rho}\langle\bar{u}\rangle\frac{\partial}{\partial z}\left(\rho\langle\overline{w}\rangle\right)-\langle\bar{v}\rangle\frac{\partial}{\partial y}\langle\bar{u}\rangle-\langle\bar{w}\rangle\frac{\partial}{\partial z}\langle\bar{u}\rangle\\&=-\langle\bar{v}\rangle\frac{\partial}{\partial y}\langle\bar{u}\rangle-\langle\bar{w}\rangle\frac{\partial}{\partial z}\langle\bar{u}\rangle\end{aligned}$$

Similarly, we can rewrite eddy flux divergence of temperature

$$-\frac{\partial}{\partial y}\left(\bar{v}\bar{\theta}\right)-\frac{1}{\rho}\frac{\partial}{\partial z}\left(\rho\bar{w}\bar{\theta}\right)=-\langle\bar{v}\rangle\frac{\partial}{\partial y}\left\langle\bar{\theta}\right\rangle-\langle\bar{w}\rangle\frac{\partial}{\partial z}\left\langle\bar{\theta}\right\rangle-\frac{\partial}{\partial y}\left\langle\tilde{\bar{v}}\tilde{\bar{\theta}}\right\rangle-\frac{1}{\rho}\frac{\partial}{\partial z}\left\langle\rho\tilde{\bar{w}}\tilde{\bar{\theta}}\right\rangle \tag{54}$$

Finally, we conclude with the planetary/intraseasonal scale system after time averaging on Eqs. (48-50) plus Eqs. (38b, 38d)

$$\frac{D}{DT}\langle\bar{u}\rangle-y\langle\bar{v}_2\rangle=-\langle\bar{p}\rangle_X-d\langle\bar{u}\rangle-\frac{\partial}{\partial y}\left\langle\overline{v'u'}\right\rangle-\frac{1}{\rho}\frac{\partial}{\partial z}\left(\rho\left\langle\overline{w'u'}\right\rangle\right)-\frac{\partial}{\partial y}\left\langle\tilde{\bar{v}}\tilde{\bar{u}}\right\rangle-\frac{1}{\rho}\frac{\partial}{\partial z}\left(\rho\left\langle\tilde{\bar{w}}\tilde{\bar{u}}\right\rangle\right)+\left\langle\bar{S}_{u,2}\right\rangle \tag{55a}$$

$$y\langle\bar{u}\rangle=-\langle\bar{p}\rangle_y+\left\langle\bar{S}_v\right\rangle \tag{55b}$$

$$\frac{D}{DT}\left\langle\bar{\theta}\right\rangle+N^2\langle\bar{w}_2\rangle=-d_\theta\left\langle\bar{\theta}\right\rangle-\frac{\partial}{\partial y}\left\langle\overline{v'\theta'}\right\rangle-\frac{1}{\rho}\frac{\partial}{\partial z}\left(\rho\left\langle\overline{w'\theta'}\right\rangle\right)-\frac{\partial}{\partial y}\left\langle\tilde{\bar{v}}\tilde{\bar{\theta}}\right\rangle-\frac{1}{\rho}\frac{\partial}{\partial z}\left(\rho\left\langle\tilde{\bar{w}}\tilde{\bar{\theta}}\right\rangle\right)+\left\langle\bar{S}_{\theta,2}\right\rangle \tag{55c}$$

$$\langle \bar{p} \rangle_z = \langle \bar{\theta} \rangle \tag{55d}$$

$$\langle \bar{u} \rangle_X + \langle \bar{v}_2 \rangle_y + \frac{1}{\rho} \left(\rho \langle \bar{w}_2 \rangle \right)_z = 0 \tag{55e}$$

where $\frac{D}{DT} = \frac{\partial}{\partial T} + \langle \bar{v} \rangle \frac{\partial}{\partial y} + \langle \bar{w} \rangle \frac{\partial}{\partial z}$, thus this system is advected by the leading-order meridional and vertical velocities on the planetary/intraseasonal scales. Now, the derivation of the multi-scale model is complete.

B Explicit formulas for the eddy flux divergences of momentum and temperature

The following formulas are the explicit solutions for Eqs. (16a-16e) corresponding to the simple heating profile (Eq. 19) in the first two baroclinic modes

$$\begin{pmatrix} p \\ u \\ v \\ \theta \\ w \end{pmatrix} = \begin{pmatrix} \left[\tilde{p}_{0|1}(y) + \gamma \tilde{p}_{1|1}(y)\right] \cos(kX + \omega t) \cos(z) \\ \left[\tilde{u}_{0|1}(y) + \gamma \tilde{u}_{1|1}(y)\right] \cos(kX + \omega t) \cos(z) \\ \left[\tilde{v}_{0|1}(y) + \gamma \tilde{v}_{1|1}(y)\right] \sin(kX + \omega t) \cos(z) \\ \left[\tilde{\theta}_{0|1}(y) + \gamma \tilde{\theta}_{1|1}(y)\right] \cos(kX + \omega t) \sin(z) \\ \left[\tilde{w}_{0|1}(y) + \gamma \tilde{w}_{1|1}(y)\right] \sin(kX + \omega t) \sin(z) \end{pmatrix} + \alpha \begin{pmatrix} \left[\tilde{p}_{0|2}(y) + \gamma \tilde{p}_{1|2}(y)\right] \cos(kX + \omega t + \beta) \cos(2z) \\ \left[\tilde{u}_{0|2}(y) + \gamma \tilde{u}_{1|2}(y)\right] \cos(kX + \omega t + \beta) \cos(2z) \\ \left[\tilde{v}_{0|2}(y) + \gamma \tilde{v}_{1|2}(y)\right] \sin(kX + \omega t + \beta) \cos(2z) \\ \left[\tilde{\theta}_{0|2}(y) + \gamma \tilde{\theta}_{1|2}(y)\right] \cos(kX + \omega t + \beta) \sin(2z) \\ \left[\tilde{w}_{0|2}(y) + \gamma \tilde{w}_{1|2}(y)\right] \sin(kX + \omega t + \beta) \sin(2z) \end{pmatrix} \tag{56}$$

Since it can be proved that the homogeneous solutions of Eqs. (16a-16e) do not contribute to eddy flux divergences of momentum and temperature F^u, F^θ, here we only show the particular solutions corresponding to the prescribed heating (Eq. 19). For a simple heating profile with the leading two parabolic cylinder functions as its meridional profiles, $\tilde{p}_{0|q}, \tilde{u}_{0|q}, \tilde{v}_{0|q}, \tilde{\theta}_{0|q}, \tilde{w}_{0|q}$,$\tilde{p}_{1|q}, \tilde{u}_{1|q}, \tilde{v}_{1|q}, \tilde{\theta}_{1|q}, \tilde{w}_{1|q}$ in the expression (56) can be rewritten as follows

$$\begin{pmatrix} \tilde{p}_{0|q} \\ \tilde{u}_{0|q} \\ \tilde{v}_{0|q} \\ \tilde{\theta}_{0|q} \\ \tilde{w}_{0|q} \end{pmatrix} = \begin{pmatrix} \left(-\frac{\sqrt{2}}{6\omega} - \frac{\sqrt{2}\omega}{6\left(\frac{3N}{q} - \omega^2\right)}\right) \phi_{2|q} + \left(-\frac{5}{6\omega} + \frac{\omega}{6\left(\frac{3N}{q} - \omega^2\right)}\right) \phi_{0|q} \\ \left(-\frac{\sqrt{2}q}{6\omega N} - \frac{\sqrt{2}q\omega}{6N\left(\frac{3N}{q} - \omega^2\right)}\right) \phi_{2|q} + \left(-\frac{q}{6\omega N} - \frac{q\omega}{6N\left(\frac{3N}{q} - \omega^2\right)}\right) \phi_{0|q} \\ \sqrt{\frac{q}{2N}} \frac{1}{\frac{3N}{q} - \omega^2} \phi_{1|q} \\ \left(\frac{\sqrt{2}q}{6\omega} + \frac{\sqrt{2}q\omega}{6\left(\frac{3N}{q} - \omega^2\right)}\right) \phi_{2|q} + \left(\frac{5q}{6\omega} - \frac{q\omega}{6\left(\frac{3N}{q} - \omega^2\right)}\right) \phi_{0|q} \\ \left(\frac{q}{3\sqrt{2}N^2} + \frac{q\omega^2}{3\sqrt{2}N^2\left(\frac{3N}{q} - \omega^2\right)}\right) \phi_{2|q} + \left(-\frac{q}{6N^2} - \frac{q\omega^2}{6N^2\left(\frac{3N}{q} - \omega^2\right)}\right) \phi_{0|q} \end{pmatrix} \tag{57}$$

$$\begin{pmatrix} \tilde{p}_{1|q} \\ \tilde{u}_{1|q} \\ \tilde{v}_{1|q} \\ \tilde{\theta}_{1|q} \\ \tilde{w}_{1|q} \end{pmatrix} = \begin{pmatrix} \left(-\frac{\sqrt{6}}{10\omega} - \frac{\sqrt{6}\omega}{10\left(\frac{5N}{q} - \omega^2\right)}\right) \phi_{3|q} + \left(-\frac{3}{10\omega} + \frac{\omega}{5\left(\frac{5N}{q} - \omega^2\right)} - \frac{\omega}{2\left(\omega^2 - \frac{N}{q}\right)}\right) \phi_{1|q} \\ \left(-\frac{\sqrt{6}q}{10\omega N} - \frac{\sqrt{6}q\omega}{10N\left(\frac{5N}{q} - \omega^2\right)}\right) \phi_{3|q} + \left(\frac{3q}{10\omega N} - \frac{q\omega}{5N\left(\frac{5N}{q} - \omega^2\right)} - \frac{q\omega}{2N\left(\omega^2 - \frac{N}{q}\right)}\right) \phi_{1|q} \\ \sqrt{\frac{q}{N}} \frac{1}{\frac{5N}{q} - \omega^2} \phi_{2|q} + \sqrt{\frac{q}{2N}} \frac{1}{\omega^2 - \frac{N}{q}} \phi_{0|q} \\ \left(\frac{\sqrt{6}q}{10\omega} + \frac{\sqrt{6}q\omega}{10\left(\frac{5N}{q} - \omega^2\right)}\right) \phi_{3|q} + \left(\frac{3q}{10\omega} - \frac{q\omega}{5\left(\frac{5N}{q} - \omega^2\right)} + \frac{q\omega}{2\left(\omega^2 - \frac{N}{q}\right)}\right) \phi_{1|q} \\ \left(\frac{\sqrt{6}q}{10N^2} + \frac{\sqrt{6}q\omega^2}{10N^2\left(\frac{5N}{q} - \omega^2\right)}\right) \phi_{3|q} + \left(-\frac{7q}{10N^2} - \frac{q\omega^2}{5N^2\left(\frac{5N}{q} - \omega^2\right)} + \frac{q\omega^2}{2N^2\left(\omega^2 - \frac{N}{q}\right)}\right) \phi_{1|q} \end{pmatrix} \tag{58}$$

For a more general heating profile $\tilde{\tilde{S}}_\theta$ with an arbitrary meridional profile, we need to decompose it into different parabolic cylinder functions $\phi_{m|q}, m = 1, 2; q = 1, 2$ and calculate the corresponding solutions.

Since the eddy flux divergences of momentum and temperature F^u, F^θ are product of two physical variables after time averaging on the daily time scale, we need to apply the following facts $\langle \sin^2(\omega t) \rangle = \langle \cos^2(\omega t) \rangle = \frac{1}{2}$. Finally, we can get analytic expressions for F^u, F^θ as follows

$$\begin{aligned} F^u &= -\frac{\partial}{\partial y} \langle \tilde{\tilde{v}} \tilde{\tilde{u}} \rangle - \frac{1}{\rho} \frac{\partial}{\partial z} \left(\rho \langle \tilde{\tilde{w}} \tilde{\tilde{u}} \rangle \right) \\ &= \alpha \sin(\beta) \left\{ -\frac{\partial}{\partial y} \left[\frac{\left(\tilde{u}_{0|1} + \gamma \tilde{u}_{1|1}\right)\left(\tilde{v}_{0|2} + \gamma \tilde{v}_{1|2}\right) - \left(\tilde{u}_{0|2} + \gamma \tilde{u}_{1|2}\right)\left(\tilde{v}_{0|1} + \gamma \tilde{v}_{1|1}\right)}{4} \right] \right. \\ &\left. - \frac{1}{4}\left(\tilde{u}_{0|1} + \gamma \tilde{u}_{1|1}\right)\left(\tilde{w}_{0|2} + \gamma \tilde{w}_{1|2}\right) - \frac{1}{4}\left(\tilde{u}_{0|2} + \gamma \tilde{u}_{1|2}\right)\left(\tilde{w}_{0|1} + \gamma \tilde{w}_{1|1}\right) \right\} \cos(z) \\ &+ \alpha \sin(\beta) \left\{ -\frac{\partial}{\partial y} \left[\frac{\left(\tilde{u}_{0|1} + \gamma \tilde{u}_{1|1}\right)\left(\tilde{v}_{0|2} + \gamma \tilde{v}_{1|2}\right) - \left(\tilde{u}_{0|2} + \gamma \tilde{u}_{1|2}\right)\left(\tilde{v}_{0|1} + \gamma \tilde{v}_{1|1}\right)}{4} \right] \right. \\ &\left. - \frac{3}{4}\left(\tilde{u}_{0|1} + \gamma \tilde{u}_{1|1}\right)\left(\tilde{w}_{0|2} + \gamma \tilde{w}_{1|2}\right) + \frac{3}{4}\left(\tilde{u}_{0|2} + \gamma \tilde{u}_{1|2}\right)\left(\tilde{w}_{0|1} + \gamma \tilde{w}_{1|1}\right) \right\} \cos(3z) \end{aligned} \tag{59}$$

$$
\begin{aligned}
F^{\theta} &= -\frac{\partial}{\partial y}\left\langle \tilde{\bar{v}}\tilde{\bar{\theta}}\right\rangle - \frac{1}{\rho}\frac{\partial}{\partial z}\left(\rho\left\langle \tilde{\bar{w}}\tilde{\bar{\theta}}\right\rangle\right) \\
&= \alpha\sin(\beta)\left\{\frac{\partial}{\partial y}\left[\frac{\left(\tilde{v}_{0|1}+\gamma\tilde{v}_{1|1}\right)\left(\tilde{\theta}_{0|2}+\gamma\tilde{\theta}_{1|2}\right)+\left(\tilde{v}_{0|2}+\gamma\tilde{v}_{1|2}\right)\left(\tilde{\theta}_{0|1}+\gamma\tilde{\theta}_{1|1}\right)}{4}\right]\right. \\
&\left.-\frac{1}{4}\left(\tilde{w}_{0|1}+\gamma\tilde{w}_{1|1}\right)\left(\tilde{\theta}_{0|2}+\gamma\tilde{\theta}_{1|2}\right)+\frac{1}{4}\left(\tilde{w}_{0|2}+\gamma\tilde{w}_{1|2}\right)\left(\tilde{\theta}_{0|1}+\gamma\tilde{\theta}_{1|1}\right)\right\}\sin(z) \\
&+\alpha\sin(\beta)\left\{\frac{\partial}{\partial y}\left[\frac{\left(\tilde{v}_{0|1}+\gamma\tilde{v}_{1|1}\right)\left(\tilde{\theta}_{0|2}+\gamma\tilde{\theta}_{1|2}\right)-\left(\tilde{v}_{0|2}+\gamma\tilde{v}_{1|2}\right)\left(\tilde{\theta}_{0|1}+\gamma\tilde{\theta}_{1|1}\right)}{4}\right]\right. \\
&\left.+\frac{3}{4}\left(\tilde{w}_{0|1}+\gamma\tilde{w}_{1|1}\right)\left(\tilde{\theta}_{0|2}+\gamma\tilde{\theta}_{1|2}\right)-\frac{3}{4}\left(\tilde{w}_{0|2}+\gamma\tilde{w}_{1|2}\right)\left(\tilde{\theta}_{0|1}+\gamma\tilde{\theta}_{1|1}\right)\right\}\sin(3z)
\end{aligned}
\tag{60}
$$

C The numerical method to solve the fully coupled planetary/intraseasonal scale system

In section (4.3), we need to solve the planetary/intraseasonal scale system advected by the Hadley cell. To be brief, we rename all physical variables $u=\langle\bar{u}\rangle, p=\langle\bar{p}\rangle, \theta=\langle\bar{\theta}\rangle, v=\langle\bar{v}_2\rangle, w=\langle\bar{w}_2\rangle$ and the Hadley cell flow field $V=\langle\bar{v}\rangle, W=\langle\bar{w}\rangle$. The equations are as follows

$$\frac{\partial}{\partial T}u+V\frac{\partial}{\partial y}u+W\frac{\partial}{\partial z}u-yv=-du+F^{u} \tag{61a}$$

$$yu=-p_y \tag{61b}$$

$$\frac{\partial}{\partial T}\theta+V\frac{\partial}{\partial y}\theta+W\frac{\partial}{\partial z}\theta+N^2w=-d_{\theta}\theta+F^{\theta} \tag{61c}$$

$$p_z=\theta \tag{61d}$$

$$v_y+\frac{1}{\rho}(\rho w)_z=0 \tag{61e}$$

This system is advected by the meridional and vertical velocity $\langle\bar{v}\rangle, \langle\bar{w}\rangle$ in the model for the Hadley cell (23a-23c). We assume rigid lid boundary conditions at top and bottom of the troposphere,

$$w(X,T,y,z)\mid_{z=0,\pi}=0 \tag{62}$$

where in dimensionless unit $z=0$ represents the surface of the earth and $z=\pi$ represents the top of the troposphere.

Since we want to get the solutions in equilibrium, we can neglect the time derivatives and only solve time-independent equations. We utilize a very crucial property that both the meridional velocity and vertical velocity $\langle\bar{v}\rangle, \langle\bar{w}\rangle$ of the Hadley cell are in the first baroclinic mode, as prescribed in (25,26). Therefore, we can still use the ansatz that the solution can be represented by the sum of different baroclinic modes and the barotropic mode. The basic idea follows the numerical method used in [4]. However, due to the advection terms in this system, different vertical modes are coupled to each other. After doing vertical decomposition to separate all physical variables into different vertical modes, we use the Galerkin method to guarantee that all the equations are satisfied for a finite set of parabolic cylinder functions.

First, we do vertical decomposition and use the following ansatz

$$
\begin{cases}
u=\sum_{q=0}^{N}U_q\cos(qz); & V=H(y)\cos(z) \\
p=\sum_{q=0}^{N}P_q\cos(qz); & W=K(y)[-\sin(z)] \\
v=\sum_{q=0}^{N}V_q\cos(qz); & d=0.7; d_{\theta}=0.23 \\
\theta=\sum_{q=1}^{N}\Theta_q[-q\sin(qz)]; & F^{u}=S_1^{u}(y)\cos(z)+S_3^{u}(y)\cos(3z) \\
w=\sum_{q=1}^{N}W_q[-q\sin(qz)]; & F^{\theta}=S_1^{\theta}(y)[-\sin(z)]+S_3^{\theta}(y)[-3\sin(3z)]
\end{cases}
\tag{63}
$$

here $H(y), K(y), S_1^{u}(y), S_3^{u}(y), S_1^{\theta}(y), S_3^{\theta}(y)$ are all known functions of y. Then we can derive equations for the coefficients of all vertical modes. Here we just list equations for the q^{th} baroclinic mode, we omit the equations for the barotropic mode, the first baroclinic mode and the last baroclinic mode for simplicity.

If$q\geq 2$ and $q\leq N$, the q^{th} baroclinic mode

$$\frac{1}{2}H\frac{\partial}{\partial y}U_{q-1}+\frac{1}{2}H\frac{\partial}{\partial y}U_{q+1}-\frac{q-1}{2}KU_{q-1}+\frac{q+1}{2}KU_{q+1}-yV_q=-dU_q+S_q^{u} \tag{64}$$

$$yU_q=-\frac{\partial}{\partial y}P_q \tag{65}$$

$$\frac{q-1}{2}H\frac{\partial}{\partial y}\Theta_{q-1}+\frac{q+1}{2}H\frac{\partial}{\partial y}\Theta_{q+1}-\frac{(q-1)^2}{2}K\Theta_{q-1}+\frac{(q+1)^2}{2}K\Theta_{q+1}+qW_q=-d_\theta q\Theta_q+qS_q^\theta \tag{66}$$

$$P_q=\Theta_q \tag{67}$$

$$\frac{\partial}{\partial y}V_q-q^2W_q=0 \tag{68}$$

Now we do the meridional decomposition. Remembering that Eqs. (64-68) can be reduced to three equations for each baroclinic mode, we only need to do meridional decomposition for $U_q,P_q,V_q;q\geq 1$ as follows

$$\begin{cases} U_q=\sum\limits_{m=0}^{M-1}U_{m|q}\phi_{m|q}\left(y\right);\ S_q^u=\sum\limits_{m=0}^{M-1}S_{m|q}^u\phi_{m|q}\left(y\right) \\ P_q=\sum\limits_{m=0}^{M-1}P_{m|q}\phi_{m|q}\left(y\right);\ S_q^\theta=\sum\limits_{m=0}^{M-1}S_{m|q}^\theta\phi_{m|q}\left(y\right) \\ V_q=\sum\limits_{m=0}^{M-1}V_{m|q}\phi_{m|q}\left(y\right); \\ \Theta_q=P_q; \\ W_q=\frac{1}{q^2}\frac{\partial}{\partial y}V_q; \end{cases} \tag{69}$$

We can notice that different baroclinic modes are interacted with each other in Eqs. (64-68). In order to use the spectrum expansion techniques [4], we need to use the parabolic cylinder functions corresponding to the same baroclinic mode. Therefore, to a good approximation, we introduce the notation $\langle\cdot,\cdot\rangle$ to represent the integral from $-\infty$ to ∞ and do Galerkin projection

$$\left\langle f\left(y\right),g\left(y\right)\right\rangle=\int_{-\infty}^{\infty}f\left(y\right)g\left(y\right)dy \tag{70}$$

What we do next is to solve the equations and guarantee that the coefficients before parabolic cylinder functions are zero in each equation. Ideally, with more meridional modes, the solutions are more accurate. Here we truncate the series of the parabolic cylinder functions and choose the number of the basic functions to be large ($M=30$). Similarly, we just list equations for the q^{th} baroclinic mode, we omit the equations for the barotropic mode, the first baroclinic mode and the last baroclinic mode for simplicity.

If $q\geq 2$ and $q\leq N$, the q^{th} baroclinic mode

$$\begin{aligned} &\sum_{s=0}^{M-1}P_{s|q-1}\left\langle\frac{q-1}{2}H\frac{\partial}{\partial y}\phi_{s|q-1},\phi_{m|q}\right\rangle+\sum_{s=0}^{M-1}P_{s|q+1}\left\langle\frac{q+1}{2}H\frac{\partial}{\partial y}\phi_{s|q+1},\phi_{m|q}\right\rangle+ \\ &\sum_{s=0}^{M-1}P_{s|q-1}\left\langle-\frac{(q-1)^2}{2}K\phi_{s|q-1},\phi_{m|q}\right\rangle+\sum_{s=0}^{M-1}P_{s|q+1}\left\langle\frac{(q+1)^2}{2}K\phi_{s|q+1},\phi_{m|q}\right\rangle+ \\ &\sum_{s=0}^{M-1}U_{s|q-1}\left\langle\frac{1}{2}H\frac{\partial}{\partial y}\phi_{s|q-1},\phi_{m|q}\right\rangle+\sum_{s=0}^{M-1}U_{s|q+1}\left\langle\frac{1}{2}H\frac{\partial}{\partial y}\phi_{s|q+1},\phi_{m|q}\right\rangle+ \\ &\sum_{s=0}^{M-1}U_{s|q-1}\left\langle-\frac{q-1}{2}K\phi_{s|q-1},\phi_{m|q}\right\rangle+\sum_{s=0}^{M-1}U_{s|q+1}\left\langle\frac{q+1}{2}K\phi_{s|q+1},\phi_{m|q}\right\rangle+ \\ &\frac{1}{q}V_{m-1|q}\left(-\sqrt{2qm}\right)+d_\theta qP_{m|q}+dU_{m|q}= \\ &qS_{m|q}^\theta+S_{m|q}^u \end{aligned} \tag{71}$$

$$\begin{aligned} &\sum_{s=0}^{M-1}P_{s|q-1}\left\langle\frac{q-1}{2}H\frac{\partial}{\partial y}\phi_{s|q-1},\phi_{m|q}\right\rangle+\sum_{s=0}^{M-1}P_{s|q+1}\left\langle\frac{q+1}{2}H\frac{\partial}{\partial y}\phi_{s|q+1},\phi_{m|q}\right\rangle+ \\ &\sum_{s=0}^{M-1}P_{s|q-1}\left\langle-\frac{(q-1)^2}{2}K\phi_{s|q-1},\phi_{m|q}\right\rangle+\sum_{s=0}^{M-1}P_{s|q+1}\left\langle\frac{(q+1)^2}{2}K\phi_{s|q+1},\phi_{m|q}\right\rangle+ \\ &\sum_{s=0}^{M-1}U_{s|q-1}\left\langle-\frac{1}{2}H\frac{\partial}{\partial y}\phi_{s|q-1},\phi_{m|q}\right\rangle+\sum_{s=0}^{M-1}U_{s|q+1}\left\langle-\frac{1}{2}H\frac{\partial}{\partial y}\phi_{s|q+1},\phi_{m|q}\right\rangle+ \\ &\sum_{s=0}^{M-1}U_{s|q-1}\left\langle\frac{q-1}{2}K\phi_{s|q-1},\phi_{m|q}\right\rangle+\sum_{s=0}^{M-1}U_{s|q+1}\left\langle-\frac{q+1}{2}K\phi_{s|q+1},\phi_{m|q}\right\rangle+ \\ &\frac{1}{q}V_{m+1|q}\left(\sqrt{2q\left(m+1\right)}\right)+d_\theta qP_{m|q}-dU_{m|q}= \\ &qS_{m|q}^\theta-S_{m|q}^u \end{aligned} \tag{72}$$

$$\left(qP_{m+1|q}+U_{m+1|q}\right)\sqrt{2q\left(m+1\right)}-\left(qP_{m-1|q}-U_{m-1|q}\right)\sqrt{2qm}=0$$

Finally, we can get a linear equation with a matrix A involving all the coefficients $U_{m|q},P_{m|q},V_{m|q}$ for the physical variables, and a vector B involving all the coefficients $S_{m|q}^\theta,S_{m|q}^u$ for the forcings. Then we just solve this linear equation

$$AX = B \tag{73}$$

By using the ansatz for meridional and vertical decomposition (63,69), we can recover all the physical variables to be functions of y and z by using the vector X for all coefficients.

References

1. Albright, Mark D and Mock, Donald R and Recker, Ernest E and Reed, Richard J, A diagnostic study of the diurnal rainfall variation in the GATE B-scale area, Journal of the Atmospheric Sciences,38,1429–1445 (1981)
2. Benedict, James J and Randall, David A, Impacts of Idealized Air-Sea Coupling on Madden-Julian Oscillation Structure in the Superparameterized CAM,Journal of the Atmospheric Sciences, 68,1990–2008 (2011)
3. Biello, Joseph A and Majda, Andrew J,A New Multiscale Model for the Madden–Julian Oscillation, Journal of the atmospheric sciences, 62, 1694–1721 (2005)
4. Biello, Joseph A and Majda, Andrew J, Modulating synoptic scale convective activity and boundary layer dissipation in the IPESD models of the Madden–Julian oscillation, Dynamics of atmospheres and oceans, 42, 152–215 (2006)
5. Biello, Joseph A and Majda, Andrew J, Intraseasonal multi-scale moist dynamics of the tropical atmosphere, Communications in Mathematical Sciences, 8, 519–540 (2010)
6. Dai, Aiguo and Trenberth, Kevin E, The diurnal cycle and its depiction in the Community Climate System Model, Journal of Climate,17, 930–951 (2004)
7. Frenkel, Yevgeniy and Khouider, Boualem and Majda, Andrew J, Simple Multicloud Models for the Diurnal Cycle of Tropical Precipitation. Part I: Formulation and the Case of the Tropical Oceans, Journal of the Atmospheric Sciences, 68, 2169–2190 (2011)
8. Frenkel, Yevgeniy and Khouider, Boualem and Majda, Andrew J, Simple Multicloud Models for the Diurnal Cycle of Tropical Precipitation. Part II: The Continental Regime, Journal of the Atmospheric Sciences, 68, 2192–2207 (2011)
9. Frenkel, Yevgeniy and Majda, Andrew J and Khouider, Boualem, Simple models for the diurnal cycle and convectively coupled waves, Theoretical and Computational Fluid Dynamics, 27, 533–559 (2013)
10. Haertel, Patrick T and Kiladis, George N, Dynamics of 2-day equatorial waves, Journal of the atmospheric sciences, 61, 2707–2721 (2004)
11. Hendon, Harry H and Liebmann, Brant, Organization of convection within the Madden-Julian oscillation, Journal of Geophysical Research: Atmospheres (1984–2012), 99, 8073–8083 (1994)
12. Holton, James R and Hakim, Gregory J, An introduction to dynamic meteorology, Academic press (2012)
13. Houze, Robert A and Betts, Alan K, Convection in GATE, Reviews of Geophysics, 19, 541–576 (1981)
14. Johnson, Richard H and Rickenbach, Thomas M and Rutledge, Steven A and Ciesielski, Paul E and Schubert, Wayne H, Trimodal characteristics of tropical convection, Journal of climate, 12, 2397–2418 (1999)
15. Khairoutdinov, Marat and Randall, David and DeMott, Charlotte, Simulations of the atmospheric general circulation using a cloud-resolving model as a superparameterization of physical processes, Journal of the Atmospheric Sciences, 62, 2136–2154 (2005)
16. Khouider, Boualem and Majda, Andrew J, Model multi-cloud parameterizations for convectively coupled waves: Detailed nonlinear wave evolution, Dynamics of atmospheres and oceans, 42,59–80 (2006)
17. Khouider, Boualem and Majda, Andrew J, Multicloud convective parametrizations with crude vertical structure, Theoretical and Computational Fluid Dynamics, 20, 351–375 (2006)
18. Khouider, Boualem and Majda, Andrew J, A simple multicloud parameterization for convectively coupled tropical waves. Part I: Linear analysis, Journal of the atmospheric sciences, 63, 1308–1323 (2006)
19. Kikuchi, Kazuyoshi and Wang, Bin, Diurnal precipitation regimes in the global tropics, Journal of Climate, 21, 2680–2696 (2008)
20. Lin, Jia-Lin and Zhang, Minghua and Mapes, Brian, Zonal Momentum Budget of the Madden–Julian Oscillation: The Source and Strength of Equivalent Linear Damping, Journal of the atmospheric sciences, 62, 2172–2188 (2005)
21. Lin, Xin and Johnson, Richard H, Kinematic and thermodynamic characteristics of the flow over the western Pacific warm pool during TOGA COARE, Journal of the atmospheric sciences, 53, 695–715 (1996)
22. Andrew Majda, Introduction to PDEs and Waves for the Atmosphere and Ocean, American Mathematical Soc (2003)
23. Majda, Andrew J, New multiscale models and self-similarity in tropical convection, Journal of the atmospheric sciences, 64, 1393–1404 (2007)
24. Majda, Andrew J and Biello, Joseph A, A multiscale model for tropical intraseasonal oscillations, Proceedings of the National Academy of Sciences of the United States of America, 101, 4736–4741 (2004)
25. Majda, Andrew J and Klein, Rupert, Systematic multiscale models for the Tropics, Journal of the Atmospheric Sciences, 60, 393–408 (2003)
26. Mapes, Brian and Tulich, Stefan and Lin, Jialin and Zuidema, Paquita, The mesoscale convection life cycle: Building block or prototype for large-scale tropical waves, Dynamics of atmospheres and oceans, 42, 3–29 (2006)
27. McGarry, Mary M and Reed, Richard J, Diurnal variations in convective activity and precipitation during phases II and III of GATE, Monthly Weather Review, 106, 101–113 (1978)
28. Nakazawa, T, Tropical super clusters within intraseasonal variations over the western Pacific, Journal of the Meteorological Society of Japan, 66, 823–839 (1988)
29. Nesbitt, Stephen W and Zipser, Edward J, The diurnal cycle of rainfall and convective intensity according to three years of TRMM measurements, Journal of Climate, 16, 1456–1475 (2003)
30. Randall, David A and Dazlich, Donald A, Diurnal variability of the hydrologic cycle in a general circulation model, Journal of the atmospheric sciences, 48, 40–62 (1991)
31. Ray, CL, Diurnal variation of rainfall at san juan, pr 1, Monthly Weather Review, 56, 140–141 (1928)
32. Romps, David M, Rayleigh damping in the free troposphere, Journal of the Atmospheric Sciences, 71, 553–565 (2014)
33. Sato, Tomonori and Miura, Hiroaki and Satoh, Masaki and Takayabu, Yukari N and Wang, Yuqing, Diurnal cycle of precipitation in the tropics simulated in a global cloud-resolving model, Journal of Climate, 22, 4809–4826 (2009)
34. Sorooshian, S and Gao, X and Hsu, K and Maddox, RA and Hong, Y and Gupta, HV and Imam, B, Diurnal variability of tropical rainfall retrieved from combined GOES and TRMM satellite information, Journal of climate, 15, 983–1001 (2002)

35. Sperber, Kenneth R and Slingo, JM and Inness, PM and Lau, WK-M, On the maintenance and initiation of the intraseasonal oscillation in the NCEP/NCAR reanalysis and in the GLA and UKMO AMIP simulations, Climate Dynamics, 13, 769–795 (1997)
36. Takayabu, Yukari N, Spectral representation of rain profiles and diurnal variations observed with TRMM PR over the equatorial area, Geophysical research letters, 29, 25–1 (2002)
37. Tian, Baijun and Soden, Brian J and Wu, Xiangqian, Diurnal cycle of convection, clouds, and water vapor in the tropical upper troposphere: Satellites versus a general circulation model, Journal of Geophysical Research: Atmospheres (1984–2012), 109, D10101 (2004)
38. Wheeler, Matthew and Kiladis, George N, Convectively coupled equatorial waves: Analysis of clouds and temperature in the wavenumber-frequency domain, Journal of the Atmospheric Sciences, 56, 374–399 (1999)
39. Yang, Gui-Ying and Slingo, Julia, The diurnal cycle in the tropics, Monthly Weather Review, 129, 784–801 (2001)
40. Yang, Song and Smith, Eric A, Mechanisms for diurnal variability of global tropical rainfall observed from TRMM, Journal of climate, 19, 5190–5226 (2006)
41. Yanai, Michio and Chen, Baode and Tung, Wen-wen, The Madden-Julian oscillation observed during the TOGA COARE IOP: Global view, Journal of the atmospheric sciences, 57, 2374–2396 (2000)